Seismological Institute
The University
Uppsala, Sweden

Uppsala, January 27, 1965

European Office of Aerospace Research
Shell Building
47 Cantersteen
Brussels, Belgium

Sixth Semi-Annual Technical Report

(Report No. 37)

Period Covered: July 1 - December 31, 1964

Arpa Order No. 180-62, Amendment No. 7, dated 3 Aug. 1961
Project Code 8100, Program Category 015, Project 8652, Task 86520

Name of Contractor:	University of Uppsala Uppsala, Sweden
Date of Contract:	19 Feb. 1962
Contract Number:	AF 61(052)-588
Amount of Contract:	$ 19,120.00
Contract Expiration Date:	30 June 1965
Name and Phone Number of Project Scientist:	Dr. Markus Båth Seismological Institute 130258
Short Title of the Work:	Rheologic Properties of the Solid Earth.

Personnel

The following persons have been working on the contract:
Markus Båth, Project Scientist, variable part-time.
Seweryn J. Duda, full-time.

Research Status

Seweryn J. Duda spent part of the time reported in the USA completing his temporary stay at the Seismological Laboratory, Pasadena, California, and returned in September, 1964, to Sweden for research at the Seismological Institute, Uppsala.

During his stay in Pasadena S.J. Duda carried out an investigation of the regional seismicity of Arizona and of seismic wave propagation at very short epicentral distances. For this purpose the records from the seismic array station at the Tonto

Forest Seismological Observatory (TFSO) near Payson, Arizona, were used. The investigation was performed as a joint project of the Seismological Institute, Uppsala, under the present contract, and the Seismological Laboratory, Pasadena, under Contract AF-49(638)-1337.

A paper has been prepared under the title: Regional seismicity and seismic wave propagation from records at the Tonto Forest Seismological Observatory, Payson, Arizona. The paper is attached as an Appendix to the present report.

A second investigation was also continued in the time reported. This concerns the strain energy release in the circum-Pacific belt from 1897 until 1963. The investigation is essentially completed and a paper is being prepared under the title: Secular strain energy release in the circum-Pacific belt. The paper will be attached as an appendix to a Monthly Status Report in the near future.

In the following we report our investigations carried out, results obtained and activities in the following order:

1. Regional seismicity and seismic wave propagation from records at the Tonto Forest Seismological Observatory, Payson, Arizona.
2. Secular strain energy release in the circum-Pacific belt.
3. Travels and institutes visited.

1. Regional seismicity and seismic wave propagation from records at the Tonto Forest Seismological Observatory, Payson, Arizona

Copies of records of the seismic array station at Tonto Forest Seismological Observatory are stored at the Seismological Laboratory, Pasadena. Following a suggestion by Prof. Frank Press, S.J. Duda inspected the records, collecting data on earthquakes which had occurred in Arizona from Sep. 15, 1963, until Jan. 31, 1964. This

time was chosen because records and bulletins were then available.

a. Discrimination of earthquakes and explosions

In the period of 4½ months, 82 earthquakes occurred in Arizona large enough to be recorded by TFSO. The magnitudes range from -1.1 to +3.7. Only the largest earthquake was recorded outside Arizona, all others being recorded exclusively by TFSO. The epicentral distances range from 14 km to 330 km. In this distance range a considerable number of explosions was recorded, originating in the numerous quarries in Arizona. To discriminate earthquakes from explosions the following criteria were used:

(i) the position of the epicenter if compared with the position of working mines in Arizona;

(ii) the origin time of the event if related to working time and habits;

(iii) the ratio of S- to P-wave energy recorded.

The last item is explained in section c. below.

b. Seismicity of Arizona

The earthquakes in Arizona in this time interval turned out to be small in number and magnitude. Two previous investigations of the Arizona seismicity are known: Townley and Allen (1939, Descriptive Catalog of Earthquakes of the Pacific Coast of the United States, 1769 to 1928, Bull. Seism. Soc. Am., vol. 29) and Woollard (1951, Report on the Special Committee on the Geophysical and Geological Study of Continents 1950-51, Trans. Am. Geoph. Un., vol. 32). From these two publications there is no evidence of essential variations of the Arizona seismicity in the past, and the conclusion obtained from our investigation seems to characterize the seismicity of Arizona in general.

c. Wave propagation at very short epicentral distances

To extend the epicentral distance range investigated, two

earthquake sequences were included in our study: from Imperial County, California, and from Baja California. In earthquake sequences the chance to include an explosion among the earthquakes is negligible. The characteristics of the earthquake sequences were determined. The earthquakes and explosions cover the epicentral distance range from 14 km to 640 km. This allowed us to study various aspects of wave propagation at short epicentral distances.

The ratio of S- to P-wave energy from earthquakes and explosions was investigated as function of magnitude and distance of the event. Whereas no dependence on magnitude was found, the distance was shown to influence the ratio both for earthquakes and explosions. At a distance of 14 km, the ratio amounts to about 100 for earthquakes. This means that shear-wave energy is preferentially generated in the earthquake focus. The ratio shows a distinct minimum at 100 km, amounting to 10 for earthquakes and only 4 for explosions. The ratio increases with distance at a higher rate for earthquakes than for explosions. The ratio of S- to P-wave energy as function of distance displays the different attenuation of the two kinds of waves. The ratio served as one of the criteria to distinguish between earthquakes and explosions in Arizona.

d. Seismic energy of earthquakes in the magnitude range $-0.7 \leq M \leq +4.9$

The duration of the S-wave, preferentially generated at the earthquake focus, depends mainly on the magnitude. A corresponding formula was derived.

The period of the Sg-wave increases in general with distance. Rapid, possibly discontinuous increases were ascertained to occur at 100 km and about 325 km epicentral distance. This has a clear bearing on the attenuation of Sg-waves at those distances. The knowledge of the discontinuous attenuation leads to a better

estimation of the seismic energy released in an earthquake with a certain magnitude. An earlier magnitude-energy conversion formula for local earthquakes was shown to give somewhat low energy, as these discontinuities could not be taken into account.

e. Discussion of the array station

Our investigation is to our knowledge the first one where an array station was used for the study of regional seismicity and seismic wave propagation at very short epicentral distances. From our experience the main advantages of an array station over a conventional station are:

(i) the high sensitivity of the individual seismometers, the maximum magnification amounting to 1.600.000 at a period of 0.3 sec;

(ii) the possibility to improve the signal-to-noise ratio, if data are recorded on magnetic tape (in our investigation, however, only records on microfilm were available);

(iii) the regular spacing of array seismometers;

(iv) the possibility to process the data automatically;

(v) the convenience of operating the station within a relatively small area, as compared to a local network of stations in the conventional sense.

The main shortcoming of an array station for problems of the present investigation is the inaccuracy in azimuth determination despite the maximal dimension of the array. This could be overcome by increasing the maximum dimension, or still better, by operating two or more array stations at proper relative distances. This would assure the number of earthquakes to be completely recorded down to extremely low magnitudes.

f. Further plans

The investigation reported is considered as finished.

2. Secular strain energy release in the circum-Pacific belt

The investigation on the secular strain energy release in the circum-Pacific belt was started by S.J. Duda during his visit to the Seismological Laboratory, Pasadena, in cooperation with Prof. Hugo Benioff. Part of the investigation was reported in the Fifth Semi-Annual Technical Report (Report No. 30).

a. Depth classes of earthquakes

Data on earthquakes with magnitudes $M \geq 7.0$ were collected for the 67 years from 1897 to 1963 inclusive. The earthquakes were arranged in classes according to focal depth. The limiting depth between shallow and intermediate earthquakes was taken at 65 km, as usual. The limiting depth between intermediate and deep earthquakes was taken at 450 km. This is somewhat different than used hitherto, but strongly recommended from the results of an investigation of the secular strain release versus focal depth (Båth and Duda, 1963). According to this, the strain release is highest in the uppermost 75 km and decreases gradually with depth and disappears at 400 km. No activity is observed between 400 and 475 km depth. The deep-focus earthquakes in the depth range between 475 and 650 km give rise to a second maximum. Our strain release study suggests the shallow and intermediate earthquakes in the depth range 0-400 km to form one unity and the deep earthquakes in the range 475-650 km to form another. Thus it is reasonable to put the depth limit separating intermediate from deep earthquakes between 400 and 475 km, say at 450 km.

b. Intensity of strain energy release in shallow shocks

The circum-Pacific seismic belt was divided into 8 regions, each of them being defined by the clustering of epicenters. The epicenters usually lie along an arched structure and the length of the arc can be determined. Most of the seismic energy is released

in shallow shocks.

The seismic energy released in shallow shocks in every region was related to 1° of arc. This figure shows inasmuch a regularity, as the region of Japan, Kurile Islands and Kamchatka has the highest strain energy release per degree of arc, and it decreases in both directions around the circum-Pacific belt. A secondary maximum is found in South America.

c. Recurrence diagram

We found that the maximum magnitude in any region is higher the larger the strain energy release is per degree of arc in shallow shocks.

The recurrence diagram, giving the number of shocks in every magnitude class:

$$\log N = a - b M$$

where N is the number of shocks with magnitude M and a,b are constants, was determined for all circum-Pacific regions. It appears as if the b-coefficient is lowest in the region with highest strain energy release per degree of arc,i.e. in a highly prestressed medium, and, reversely, largest in the region with smallest strain energy release per degree of arc, i.e. in a medium only slightly prestressed.

This throws some new light on aftershocks. In the Kamchatka 1952 aftershock sequence (Båth and Benioff, 1958, The aftershock sequence of the Kamchatka earthquake of November 4, 1952, Bull. Seism. Soc. Am., 48, 1-15) the b-coefficient amounts to 1.5, as compared with 1.01 for the region of Japan, Kurile Islands and Kamchatka. In the Aleutian Islands 1957 aftershock sequence (Duda, 1962, Phaenomenologische Untersuchung einer Nachbebenserie aus dem Gebiet der Aleuten-Inseln, Freiberger Forschungshefte, C 132, Geoph., 1-90) the b-coefficient was found to be 1.45, as compared with 0.73 for the region of Aleutian Islands and Alaska. In both

cases the b-coefficient of aftershock sequences is larger than the secular value in the corresponding regions. This implies that the aftershocks occur in a volume with reduced prestress, if compared with the average, acting over a longer time interval in the region. This is well compatible with Benioff's hypothesis of aftershock generation.

d. Further plans

The investigation is partially written down. It is intended to be enlarged with a part concerning the strain energy release outside the circum-Pacific belt.

3. Travels performed and institutes visited

Seweryn J. Duda terminated his temporary stay at the Seismological Laboratory, Pasadena, on Sep. 10, 1964, and returned to the Seismological Institute, Uppsala, on Sep. 28, 1964. During the travel across the United States he visited some geophysicists and institutions of seismological interest in the vincinity of Boston, Mass.: Prof. F. Birch, Harvard University, Department of Experimental Geology, Cambridge, Mass.; Prof. S.M. Simpson, M.I.T., Department of Geology and Geophysics, Cambridge, Mass.; Rev. Dr. D. Linehan, S.J., Boston College, Weston Observatory, Weston, Mass.

Bibliography

The following is a complete list of technical reports prepared under the present contract up to now:

1. Båth, M., S.J. Duda: Strain release in relation to focal depth, Appendix I to the Third Semi-Annual Technical Report (Report No. 16), published in Geofisica pura e applicata, 56, 93-100, 1963.
2. Båth, M., S.J. Duda: Earthquake volume, fault plane area, seismic energy, strain, deformation and related quantities, Appendix I to the Fourth Semi-Annual Technical Report (Report No. 23),

published in Annali di Geofisica, XVII, 353-368, 1964

3. Duda, S.J.: Strain release in the circum-Pacific belt: Chile 1960, Appendix to the Ninth Monthly Status Report (Report No. 12), published in Journ. Geoph. Res., 68, 5531-5544, 1963.

4. Duda, S.J.: The stress field around a fault according to a photoelastic model experiment, Appendix II to the Fourth Semi-Annual Technical Report (Report No. 23), in press at the Geoph. Journ., 1965.

5. Duda, S.J.: Regional seismicity and seismic wave propagation from records at the Tonto Forest Seismological Observatory, Payson, Arizona, Appendix to the present Sixth Semi-Annual Technical Report (Report No. 37), intended for publication in Proceedings of the Royal Society, 1965.

6. Duda, S.J., M. Båth: Strain release in the circum-Pacific belt: Kern County 1952, Desert Hot Springs 1948, San Francisco 1957, Appendix I to the Second Semi-Annual Technical Report (Report No. 9), published in Geophys. Journ., 7, 554-570, 1963.

Financial Status

A complete account of the financial development since the beginning of the contract up to now was given in the Monthly Status Report for December, 1964 (Report No. 36).

Markus Båth
Project Scientist

A P P E N D I X

REGIONAL SEISMICITY AND SEISMIC WAVE PROPAGATION FROM RECORDS AT THE TONTO FOREST SEISMOLOGICAL OBSERVATORY, PAYSON, ARIZONA

Seweryn J. Duda

Seismological Institute

University of Uppsala

Uppsala, Sweden

Contract No. AF 61(052)-588

January 27, 1965

Prepared for

GEOPHYSICS RESEARCH DIRECTORATE

AIR FORCE CAMBRIDGE RESEARCH LABORATORIES

OFFICE OF AEROSPACE RESEARCH

UNITED STATES AIR FORCE

BEDFORD, MASSACHUSETTS

WORK SPONSORED BY ADVANCED RESEARCH PROJECTS AGENCY

PROJECT VELA-UNIFORM

ARPA Order No. 180-62, Amendment No. 7, dated 3 Aug. 1961.

Project Code 8100, Program Category 015, Project 8652, Task 86520

Intended for publication in Proceedings of the Royal Society, London.

REGIONAL SEISMICITY AND SEISMIC WAVE PROPAGATION FROM RECORDS AT THE TONTO FOREST SEISMOLOGICAL OBSERVATORY, PAYSON, ARIZONA

By SEWERYN J. DUDA

(Received January 1965)

The records of the Tonto Forest Seismological Observatory near Payson, Arizona, have been used to investigate the applicability of an array station for the study of local seismicity and seismic wave propagation at short epicentral distances. Inferences are drawn about the seismicity of Arizona and the characteristics are given for two earthquake sequences, in Imperial County, California, and in Baja California.

The records of the earthquakes and a selection of quarry blasts are used for the study of the propagation of crustal waves. According to their group velocities and appearance, the Sg- and P^*-waves observed at small epicentral distances are identical with the Lg2 and Lg-wave respectively, observed at larger epicentral distances.

The ratio of S- to P-wave energy is estimated to be of the order of 100:1 for earthquakes at an epicentral distance of about 14 km. The attenuation of Sg-wave energy has a discontinuity at an epicentral distance of 325 km and possibly another at 100 km. Because of this fact an appreciable difference of seismic energies recorded at two epicentral distances, slightly below and above these critical distances will be observed. The duration of the Sg-phase depends mainly on the magnitude of the earthquakes.

A magnitude-energy conversion formula is derived in the form:

$$\log E = 10.06 + (2.17 \pm 0.07)\, M_L$$

for the magnitude range $-0.7 \leq M_L \leq +4.9$ and the distance range

$14 \text{ km} \leq \Delta \leq 640 \text{ km}$.

1. INTRODUCTION

In the last years a new technique of recording seismic waves was introduced by seismic array stations. Due to the large magnification of the individual array seismographs, of the order of millions, as well as the possibility to increase the ratio between signal and noise, array stations offer the advantage of highest perceptibility of events. However, before the advantages and shortcomings of an array station in comparison with a conventional seismograph station can be weighed we must attempt to solve different seismological problems by means of it.

The first purpose of the present investigation is to draw methodical conclusions on the applicability of an array station for the study of regional seismicity and seismic wave propagation. The accuracy in epicentral distance and azimuth determination is estimated. The increase of the minimum recorded magnitude with epicentral distance is determined. The possibilities to find the attenuation of seismic waves are presented. From this, inferences about the optimal relative position of two or more array stations are drawn.

The second purpose of the investigation is to give several direct seismological results concerning:

1. some aspects of the seismicity of Arizona and of two earthquake sequences, in Imperial County, California (Imperial Valley) and Baja California,
2. the wave propagation at shortest epicentral distances.

The present paper is based on records from the Tonto Forest Seismological Observatory (TFSO) near Payson, Arizona.

TFSO ($34^{\circ}16'04''$ N, $111^{\circ}16'13''$ W) is situated close to the centre of Arizona (figure 1). The epicentral distance of Arizona

events recorded at TFSO lie within 3°.

The propagation of seismic waves in this distance range was investigated from records of earthquakes as well as explosions, the latter originating in the numerous quarries in some parts of Arizona.

Differences in records from earthquakes and explosions allowed a fair separation of the two kinds of events in this distance range. An epicentral map of Arizona earthquakes is presented.

In the present study two earthquake sequences were included: from Imperial County, California, and from Baja California. The epicentral distances in the first sequence range from 2.8° to 4.1°, and in the second sequence from 3.0° to 5.8°. In the case of earthquake sequences from a limited area the chance of including an explosion is negligible. The characteristics of these two earthquake sequences were found, and the study of seismic wave propagation was extended to the epicentral distance range from 2.8° to 5.8°.

2. OBSERVATIONAL DATA

2.1 Instruments and magnitudes

The seismographs at the TFSO form two arrays: an areal array with a diameter of 3.8 km, and a linear or "S-wave type" array, with a length of 10.4 km of each one of two perpendicular seismograph lines in the shape of a cross.

For our study the records of a 3-component set of seismometers situated in the centre of the array, and 4 vertical seismometers situated at the ends of the linear array were used. All seismometers operated with a maximum magnification of 1,600,000 at a period of 0.3 sec throughout the time interval investigated. On the records measured 1 sec corresponds to about 1 mm.

Figure 2 shows the frequency response characteristic of a single array seismometer (Johnson-Matheson) and that of the standard

Wood-Anderson torsion seismometer. Besides their maximum magnification, the differences in the characteristics are considered small. Therefore the magnitudes M_L of the shocks could be determined according to the original definition by Richter (1935), without the necessity of a transformation of our records into such as would be obtained by the torsion seismometer.

Table 1 lists all of our earthquakes whose magnitudes M_L were determined from the TFSO as well as from Pasadena records. The mean magnitude difference is small, and amounts to 0.2. This difference may be a result of:

(i) the above-mentioned difference in the response characteristics of the instruments used,

(ii) the radiation pattern of the earthquakes, and

(iii) the station correction needed for TFSO.

In light of the small difference in response characteristics, and the fact that the radiation pattern for small shocks is obliterated by horizontal refractions (Bune & al. 1960), the magnitude difference of 0.2 may be considered as tentative "station correction" for the horizontal seismographs, whose records were used for the magnitude determination in our study. However, the introduction of it into our calculations seems premature, since it could be based on only 8 cases.

2.2 Seismograms and accuracy

For this study the records and the TFSO-bulletins for the time from September 15, 1963, to January 31, 1964, were at our disposal. The following events were examined:

(i) all earthquakes within the epicentral distance of 3° in this time interval, amounting to 82;

(ii) a selection of 93 explosions in the distance range from 1° to 3°;

(iii) the earthquakes on October 27, 1963, in Imperial County,

California, amounting to 50; and

(iv) the earthquakes in the time from November 23 to 31, 1963, in Baja California, amounting to 64.

A shock was accepted if at least one S- and one P-wave could be identified. The Sg-phase was the most prominent in the entire epicentral distance range investigated. Magnitudes were based exclusively on Sg. Up to about 1° the Pg-phase, and beyond that distance, the additional Pn-phase, could usually be found. Sometimes, especially for stronger shocks, the P^{*}- and Sn-phases were present.

Arrival times, amplitudes and periods of the compressional phases (Pn, P^{*}, Pg) were determined from the vertical component and of the distortional phases (Sn, S^{*}, Sg) from the horizontal components of the central 3-component set of seismographs.

All independent time-differences between the phases were used in the determination of the epicentral distances.

The travel times for crustal phases at zero focal depth, as given by Jeffreys & Bullen (1958), were used. The travel times can be expected to differ from those in the investigated regions. The disagreement of epicentral distances calculated from two or more phase differences increased with epicentral distance. At 3° it was generally lower than 0.2° and reached only exceptionally 0.5° at the largest epicentral distances considered. If the local travel times were known, the accuracy of epicentral distance determination could be increased, as well as the focal depth determined. The azimuth towards the epicentre was found from the differences in arrival time of the first P-phase on the 5 vertical seismometers, situated at the very ends of the linear arrays and in the centre. The azimuths at epicentral distances up to 3° are accurate to $\pm 11.25^{\circ}$ or even less. For epicentral distances beyond 3°, however, the determination of the azimuths is more critical. The reason is that the fi[illegible] events become

difficult to identify, and no accurate time reading or phase correlation on different traces is possible (Richter 1958). The epicentres for Imperial County and Baja California in figure 1 therefore appear on a line, the azimuth being accurate to about $\pm 22.50^{\circ}$, unless the epicentre was reported by USCGS.

2.3 Perceptibility of earthquakes by the station

Figure 3 shows the magnitudes M_L of the earthquakes investigated as a function of the epicentral distance. The increase of minimum magnitude with distance is nonlinear in the epicentral distance range from 0 to about 600 km. In particular, there is a rapid increase of minimum magnitude at the shortest epicentral distances. This means that earthquakes with low magnitudes can be recorded only if the epicentre is situated close to the station.

The poor perceptibility to earthquakes with low magnitudes can be understood in terms of higher absorption of shortperiod than longperiod waves. Although the magnitude does not take into account the wave period directly, it is well known that the wave spectrum generated by earthquakes with low magnitudes has a maximum at shorter period than those for earthquakes with larger magnitudes. The shortperiod content of the spectrum of earthquakes with any magnitude is absorbed at small hypocentral distances, and at larger distances only the longperiod part can be recorded. Since the latter has a low intensity for earthquakes with small magnitudes, their range of perceptibility is small.

From the diagram in figure 3 we see immediately that the number of earthquakes can be complete only for $M_L \geq + 1.5$ in Arizona, for $M_L \geq + 2.0$ in Imperial County and for $M_L \geq + 2.7$ in Baja California.

On the other hand, the maximum magnitude which can be determined at a certain epicentral distance is limited by the magnification of the seismographs. Therefore, magnitudes could not be determined for

4 earthquakes in Imperial County and 1 earthquake in Baja California, though reported by Pasadena. There were 5 earthquakes in Arizona not recorded in Pasadena, but recorded at the TFSO with amplitudes too large to allow a magnitude determination. Most of the shocks investigated in each of the regions were recorded exclusively by the TFSO.

3. SEISMICITY

3.1. Epicentral map of Arizona

In the past the seismicity of Arizona has been investigated only sporadically. Townley and Allen (1939) published a descriptive catalog of Arizona earthquakes in the interval 1769 to 1928. Woollard (1951) presented a map with earthquake epicentres of the Rocky Mountain region from USCGS reports. This map includes 21 epicentres in Arizona for an interval of "several years" up to 1949.

In this study, high sensitivity of the seismographs causes that besides earthquakes a considerable number of artificial events. especially quarry blasts, is recorded. This raises the problem of distinguishing between earthquakes and explosions.

For Arizona events the following criteria were applied jointly to separate earthquakes from explosions:

(i) The position of the epicentre, if compared with the position of working mines in Arizona.

(ii) The origin time of the event, if related to working time and habits.

(iii) The ratio of S- to P-wave energy recorded (see Section 5.1.).

If an earthquake happened underneath a site with mines, however, it could be misinterpreted as explosion. This is true especially for the region bounded by the longitudes 110° and 111°W and latitudes 31.5° and 33.5°N, situated towards the SSE of TFSO, where many

explosions took place in the investigated time interval (figure 1). No explosions is believed to be misinterpreted as earthquake.

Figure 1 shows the epicentres of all earthquakes in Arizona in the investigated time interval. The magnitudes of 77 earthquakes lie in the range from - 0.7 to + 2.1, with a single shock of magnitude + 3.7 (table 1). There was possibly even a shock with a magnitude as low as - 1.1. However, only the Sg-phase could be identified. The epicentre of this earthquake was assumed to be identical with another one, which occurred 23 minutes earlier.

On the epicentral map a considerable scatter of epicentres is seen, which can be only partially related to the errors in epicentre determination. It appears that earthquakes with low magnitudes are distributed over most of Arizona. The seismicity was low in terms of number of shocks and their magnitudes. From the stronger shocks it is seen that besides the slightly indicated NW-SE striking belt of seismicity, as already reported by Woollard (1951), there is a branch running from the middle of Arizona towards the SW so as to meet the region of strong seismicity in Baja California.

3.2. Some tectonic features of the investigated regions

The genesis of the present seismicity of any region may be looked for in the most recent tectonic history of the region considered. Past tectonic events have importance for the present seismicity, the more the younger they are and the more intensive their appearance was.

We were looking for such characteristic features in the tectonic history of Arizona, Imperial County and Baja California, which are capable to influence the present seismicity of these regions. Some differences of the characteristic features, implying differences in the occurrence of earthquakes in the three regions are pointed out.

Arizona and Imperial County turn out to be strong relative contrasts from the point of view of the genesis of seismic activity.

Arizona, belonging partially to the Basin and Range Province, underwent the latest orogeny in the late Mesozoic and early Tertiary with considerable folding, thrusting and volcanic avtivity, the latter continuing up to very recent time. As a contrast, the adjacent coastal California, including the Imperial County, has had little volcanism since the Miocene. It is believed that the present is a time of typical orogeny in southern California. Whereas any present seismicity of Arizona may be expected to be related to orogenetic events with volcanic activity, the seismic activity in Imperial County is related to movements on the San Andreas fault system, and is probably connected with the Imperial Fault.

Baja California occupies an intermediate position. Volcanism has continued since Miocene and Pleistocene up to the present time, but Tertiary and Quaternary uplift of the peninsula, as well as faulting continuing during Quaternary along some fault zones, are known. Earthquake activity in Baja California may therefore be related to both tectonic movements and volcanic processes in the peninsula. For details of the tectonical development of the regions, see Eardley (1951).

3.3. Recurrence diagrams

The number of earthquakes in a certain magnitude range was found to increase exponentially with decreasing magnitudes (Gutenberg & Richter 1954):

$$\log n = a - bM \qquad (3 \cdot 1)$$

where n is frequency, i.e. number of earthquakes in the magnitude range $M \pm \delta M$,

M the magnitude of the earthquake, and

a,b constants.

All logarithms in this paper are to the base 10. The constants a,b

are used to characterize the seismicity of a region. The constant b is independent of the time interval and epicentral area chosen (or volume drawn by the hypocentres), and gives the relative proportion of shocks with different magnitudes. Both and b may vary in a region in course of time, as also from region to region.

The law expressed by (3·1) has been confirmed repeatedly for shocks with large magnitudes ($M \geq 6$). The question arises whether there is a lower magnitude limit for its validity. Asada (1957) found it to be valid in the magnitude range from -1 to + 5 in Japan. Sanford & Holmes (1962) found it to satisfy earthquakes with seismic energies as low as 10^7 ergs ($M_L \approx -1.4$).

From the 77 earthquakes with known magnitudes in Arizona, 46 in Imperial County and 63 in Baja California, the recurrence diagrams could be constructed.

Formula (3.1) cannot be applied if there is no earthquake for a certain magnitude inside the range considered. Since this is found in our case (figure 4), the cumulative frequencies N were calculated, giving the number of earthquakes above the magnitude M_L:

$$\log N = a' - bM_L \qquad (3 \cdot 2)$$

the b-coefficients in (3.1) and (3.2) being identical (Utsu 1961).

Figure 4 shows the frequency and cumulative frequency for our three populations of earthquakes. M_L is counted in steps of 0.1 unit each. From the cumulative frequency diagrams we see immediately that the data are incomplete below the magnitude limits already found (Section 2.3). Above these limits the cumulative frequency diagrams can be approximated by equations of the form (3.2).

For Baja California we observe two branches, approximated by the following equations:

$$\left.\begin{array}{lll} \text{branch I} & \log N = 4.96 - 0.47\, M_L & ;\ +2.7 \leq M_L \leq +3.6 \\ \text{branch II} & \log N = 7.25 - 1.11\, M_L & ;\ +3.7 \leq M_L \leq +4.5 \end{array}\right\} \quad (3\cdot3)$$

The change of slope at $M_L = 3.65$ is such that below this magnitude ($+2.7 \leq M_L \leq +3.6$) the number of shocks increases slower with decreasing magnitude than in the higher magnitude range ($+3.7 \leq M_L \leq +4.5$). In the diagram for Baja California an earthquake with magnitude $M_L = 6$ (Nov. 23, 1963, 07 50 46.3 GMT, 30.1N, 114.0W) which started the sequence, is not included. No earthquakes occurred in the magnitude range from 6.0 to 4.9. This sequence has therefore the appearance characteristic for aftershock sequences, with a magnitude difference between the main shock and the largest aftershock equal to 1.1. This is in very good agreement with the so-called Båth's law (Richter 1958). The sequence was investigated for 9 days, after which the seismic activity in the area dropped to about the level of the preceding time.

The Imperial County sequence has the appearance of an earthquake swarm with no outstanding earthquake. The cumulative frequency diagram (figure 4) can be approximated by the equations:

$$\left.\begin{array}{lll} \text{branch III} & \log N = 3.51 - 0.46\, M_L & ;\ +2.0 \leq M_L \leq +4.2 \\ \text{branch IV} & \log N = 5.92 - 1.07\, M_L & ;\ +3.8 \leq M_L \leq +4.6 \end{array}\right\} \quad (3\cdot4)$$

Here again two branches are needed for the approximation. The magnitude limits overlap in the middle of the range, with practically no importance for the approximation. The b-coefficients for Baja California and Imperial County exhibit a remarkable agreement in the corresponding magnitude ranges.

For Arizona one branch was found. The approximation, yielding:

$$\text{branch V} \qquad \log N = 3.11 - 1.21\, M_L \ ;\ +1.5 \leq M_L \leq +2.1 \quad (3\cdot5)$$

is vague, since only 20 earthquakes can be taken into account.

The most surprising conclusion from the above approximations is that the a- and b-coefficients in (3·1) can be different in the same region and time interval, but for differing magnitude ranges. The b-coefficient decreases with decreasing magnitude. The values of b found here are well comparable with those found repeatedly for greater magnitudes.

4. WAVE PROPAGATION

4.1. Phases

For the present purpose the Pn- and Sn-waves are understood as refracted dilational and distortional waves respectively travelling in the upper mantle. The Pg- and Sg-waves are assumed to be guided waves travelling in the earth's crust, their apparent surface velocity being equal to the group velocity in the crustal wave guide. Similarily, the P^*-wave is assumed as to be a guided wave.

Table 1 lists the group velocities with standard deviation for those investigated earthquakes, whose origin times and epicentres have been reported by USCGS.

We note immediately that the Pg- and Sg-velocities are lower than usually found.

The Pn- and Sn-velocities were calculated for a crustal layer with constant velocities and a thickness of 28 km, in agreement with models given by different authors (Tatel & Tuve 1955, Press 1960, Berg & al. 1960, Diment & al. 1961, Pakiser & Hill 1963). Two cases of crustal velocities were considered and the corresponding Pn- and Sn-velocities are presented in table 1:

(i) The mean velocity of the P-wave was taken as 6.34 km/sec in accordance with a finding for southern California (Richter 1958, p. 698) and the mean velocity of the S-wave was taken as 6.34 km/sec: $\sqrt{3}$ = 3.66 km/sec.

(ii) The mean velocities were taken as equal to the Pg- and Sg-velocities found for the respective profiles (Pakiser & Hill 1963).

The Pn-velocities are in both cases higher along the more southerly profile from Baja California than from Imperial County (table 1 and figure 1).

The velocities found for the Pn-wave from Imperial County under assumption (i) agree within error limits with the Pn-velocity (below 8 km/sec) in the Basin and Range Province (Pakiser 1963).

This would indicate that the mantle with anomalously low Pn-velocities terminates in Baja California.

Special care has been taken to identify the pertinent phases in all examined records. The identification is proved to have been successful in the case of the Pn-, Sn- and Pg-, Sg-phases by Poisson ratios (σ) calculated for the upper mantle and the crust respectively (table 1). The ratio (σ) is in all cases in close agreement with the ratio determined from Jeffreys & Bullen Tables (σ_{JB}). The Poisson ratio is seen to be higher in the upper mantle than in the crust.

The velocities and appearance of the crustal phases, observed in the distance range from 14 km up to more than 650 km, were used to find out if they can be related to crustal phases observed at larger epicentral distances.

The velocities of the Sg-phase, generally the strongest in our records, were 3.34 $\pm$ 0.17 km/sec for earthquakes in Baja California, 3.25 $\pm$ 0.13 km/sec for Imperial County and 3.06$\pm$ km/sec for Arizona, i.e. close to the velocity of the Lg2-phase (3.37 $\pm$ 0.04 km/sec) at larger epicentral distances (Båth 1954). This is in agreement with the idea that the Lg-phase is identical with the Sg-phase, as expressed by Press and Ewing (1952).

The P^*-phase was recorded from a number of earthquakes in

Imperial County (table 1). The mean velocity amounts to 6.28 ± 0.21 km/sec. The wave had small amplitudes in comparison to other phases and erratic occurrence. Both its velocity and appearance are close to that found by Press & Gutenberg (1956) for the Πg-wave at distances from 5.3° to 37.5° with a velocity of 6.09 ± 0.06 km/sec.

The Πg-phase has been proposed as corresponding to the Pg-phase. The Pg-phase was second in intensity in the entire distance range investigated. This is strange if indeed it should be identical with the Πg-phase. The same conclusion has been drawn previously by Båth (1962). From our observation we conclude rather that the Πg-phase at large epicentral distance is identical with the P^*-phase at small epicentral distances.

In table 2 are listed the phases which correspond to each other.

4.2. Periods of Pn-, Pg- and Sg-waves

If seismic events are recorded by a single station, even an array station, the seismograms usually differ from each other in the magnitude of the event and its epicentral distance. This makes it difficult to separate the effects of magnitude and distance. Nevertheless, in a number of cases it could be found which of these two factors is of prevailing importance.

The periods of the maximum oscillation of Pn- and Pg-waves on the vertical seismograph and of Sg-waves on the horizontal seismographs were measured, together with the corresponding amplitudes. As only slight changes of period with time were observed, the periods correspond in general to most of the wave train of each phase.

The periods of the Pn-, Pg-, and Sg-waves as function of magnitude display a large scatter. We conclude that the influence of the magnitude of the earthquake on the period of the maximum oscillation of each phase is below the measuring accuracy or is masked by another factor.

The periods as function of epicentral distance reveal a general increase with distance, as seen in figure 5. The dashed lines are overall least square approximations, their equations being shown in table 3.

The Pn-period is practically constant within the distance ranges from 100 km to 300 km, and from 300 km to 650 km as indicated by the small correlation coefficients shown in table 3 for the Pn-period in both distance ranges.

The Pg-period increases with distance up to 100 km, remains fairly constant between 100 km and 300 km epicentral distance (small correlation coefficient), and increases thereafter.

The Sg-period is constant in the range from 14 km to 100 km, where it jumps 0.15 sec, and remains constant up to 300 km. Here it starts to scatter strongly and increase rapidly with distance, meeting the periods found for Lg-waves (Båth 1962). If the critical distance for the Sg-wave is chosen at 350 km instead of 300 km, even a jump of the period by a factor of 2 is indicated by the data. However, we kept in all cases the critical distance for the least square approximation at 300 km, the changes of slope or jumps at that distance in the period-distance diagrams supporting each other for all three kinds of waves.

The period discontinuities of Pn, Pg and Sg at 100 km and about 300 km should have a bearing on the energy attenuation of these waves (see Section 5.2.)

No dispersion for Sg-waves could be ascertained. Thus, the large scatter of Sg-periods of distances greater than 300-350 km must be due to another factor.

The period of the P^{*}-wave, which was recorded especially from earthquakes in Imperial County, was fairly constant for distances from about 300 to 450 km and amounted to 0.40 ± 0.05 sec.

No difference in periods from earthquakes and explosions was found.

4.3. Duration of the Sg-phase

We define the duration of the wave train t_Δ at the epicentral distance Δ as the time from the beginning of the corresponding phase up to the decrease of its amplitude below 1/e ($\approx 1/3$) of its maximum value. The duration was measured for the Sg- and Pg-waves. The measurements can only be approximate due to the complexity of the records.

Whereas the duration of the Sg- and Pg-waves as function of epicentral distance display a large scatter, a clear dependence of the Sg-phase on the magnitude could be found, as shown in figure 6. A least square approximation of the data yields:

$$\log t_\Delta(Sg) = 0.254 + (0.391 \pm 0.016)\, M_L \qquad (4 \cdot 1)$$

in the magnitude range $-0.7 \leq M_L \leq +4.3$ and where $t_\Delta(Sg)$ is expressed in sec. The equation is shown as a solid line in figure 6.

The duration data were arranged according to distance classes of 50 km. In all distance classes the same relation of duration to magnitude was found. This is in agreement with Gutenberg and Richter (1956 a). Thus, the duration of the Sg-phase is independent of distance in the investigated range:

$$t_\Delta(Sg) = t_K(Sg). \qquad (4 \cdot 2)$$

K is any distance in the range considered.

No corresponding least square approximation for the duration of the Pg-phase seems justified, because of a considerable scatter of the data. As no contrary information is found, we shall assume in the following that the ratio of the duration of the Sg-phase to the duration of the Pg-phase, $t_\Delta(Sg)/t_\Delta(Pg)$, is independent of magnitude.

There are three possible factors which may influence the duration of the Sg-phase:

(i) dispersion,

(ii) attenuation

(iii) source mechanism

(iv) lateral refraction and reflexion.

If dispersion of the Sg-phase is present, even with no measurable change of period as in the case of a dispersion curve almost parallel to the velocity axis, the duration increases with epicentral distance. The attenuation of the Sg-phase diminishes the duration of the wave train with epicentral distance. As no change of the Sg-wave duration with distance was found, the factors mentioned either annihilate each other or their ratio is independent of the epicentral distance.

Therefore the increase of Sg-wave duration with magnitude is probably due to items (iii) and(iv). The duration of the Sg-wave is longer than any reasonable duration of rupture along the fault plane during an earthquake with magnitude M_L. The problem of the duration of seismic wave trains is old and no satisfactory explanation has been presented so far. Different hypotheses have been proposed or excluded (Jeffreys 1931, Tatel & Tuve 1954, Tatel 1954). A final judgement requires a special study.

5. WAVE ENERGY

5.1. Ratio of Sg- to Pg-wave energy

The seismic wave energy from a point source in a homogeneous medium, recorded at a distance h, equal to the focal depth of the source is:

$$E_h(x) = 2\pi^3 \rho\, h^2\, v(x) \int_0^{t_h(x)} \left[\frac{\bar{A}_h(x)}{T_h(x)}\right]^2 dt \qquad (5 \cdot 1)$$

where (x) refers to the kind of wave considered,

$v(x)$ is the group velocity of the corresponding wave,

$t_h(x)$ the duration of the wave train at distance h,

$\bar{A}_h(x)$, $T_h(x)$ the amplitude and the period of the wave at distance h,

ρ the density of the medium (Gutenberg & Richter 1942, 1956a,b).

In formula (5 · 1) allowance is made for the mean kinetic and potential energies in the wave train and the effect of the free surface. Assuming that no absorption takes place on the way from the focus up to a distance h, the formula gives the seismic energy radiated from the source.

The Sg- and Pg-waves carried most of the seismic energy in all investigated shocks.

The maximum amplitudes A_Δ were measured within 10 sec at most after the beginning of the phase together with the corresponding periods T_Δ. We used the horizontal component of the Sg-wave and the vertical component of the Pg-wave. It is reasonable to assume for Sg-waves that the vertical component is half of the resultant horizontal component, and for the Pg-waves that the vertical and horizontal components are equal. We then get for the ratio of the total amplitudes $\bar{A}_\Delta(x)$ to the measured amplitudes $A_\Delta(x)$:

$$k(Sg) = \frac{\bar{A}_\Delta(Sg)}{A_\Delta(Sg)} = 1.12 \qquad (5 \cdot 2)$$

$$k(Pg) = \frac{\bar{A}_\Delta(Pg)}{A_\Delta(Pg)} = 1.41 \qquad (5 \cdot 3)$$

The duration t_Δ of the wave trains was measured until the amplitude decreased below 1/e of its maximum value (see Section 4.3). We assume that the energy deficit from taking only that part of the wave train into account is compensated by the energy surplus from taking the maximum

amplitude throughout the entire duration t_Δ.

The energy of the Sg- and Pg-waves at distance h will then be:

$$E_h(Sg) = 2\pi^3 \rho h^2 v(Sg) \left[\frac{A_h(Sg)}{T_h(Sg)}\right]^2 t_h(Sg) \left[k(Sg)\right]^2 \qquad (5 \cdot 4)$$

$$E_h(Pg) = 2\pi^3 \rho h^2 v(Pg) \left[\frac{A_h(Pg)}{T_h(Pg)}\right]^2 t_h(Pg) \left[k(Pg)\right]^2 \qquad (5 \cdot 5)$$

If A_Δ, T_Δ and t_Δ are known as functions of distance, the energy at the source E_h can be calculated from the energy E_Δ recorded at epicentral distance Δ.

Figure 7 shows the ratio of the maximum particle velocities, A_Δ/T_Δ, for Sg- and Pg-waves as a function of epicentral distance. Under the above assumptions, this ratio is proportional to the square root of the ratio of the Sg-wave energy, $E_\Delta(Sg)$, to the Pg-wave energy, $E_\Delta(Pg)$:

$$\frac{A_\Delta(Sg)/T_\Delta(Sg)}{A_\Delta(Pg)/T_\Delta(Pg)} = \left[\frac{v(Pg)}{v(Sg)} \cdot \frac{t_\Delta(Pg)}{t_\Delta(Sg)}\right]^{\frac{1}{2}} \cdot \frac{k(Pg)}{k(Sg)} \left[\frac{E_\Delta(Sg)}{E_\Delta(Pg)}\right]^{\frac{1}{2}} \qquad (5 \cdot 6)$$

As this ratio is composed by 4 values determined by measurement, it will scatter. Nevertheless, averaging the ratio in intervals of 50 km epicentral distance reveals some characteristic features:

(i) The ratio (5 · 6) amounts to about 8:1 close to the epicentre and at a distance of about 600 km. In the first case this must be related to the focal process, in the second to the different propagation of the two kinds of waves.

(ii) The ratio (5 · 6) has as distinct minimum equal to 2:1 at about 100 km.

The general trend of the curves in figure 7 can be given the

following explanations, arranged in order of probable importance:

(i) Different attenuation of Pg and Sg, the Sg-attenuation being the strongest in the first 100 km but decreasing below the value of the Pg-attenuation at greater distances. This seems likely considering the large percentage of high-frequency motion in Sg close to the source.

(ii) The minimum around 100 km distance can partly be traced back to the corresponding period increase of 0.15 sec at that distance for Sg with no corresponding period change for Pg (figure 5). This period jump will cause the ratio (5 · 6) to decrease to 0.6 of its previous value.

(iii) Constructive interference between Pg, Pn and P^* at the cross-over distance near 100 km could increase the P-wave amplitude and thus contribute to the minimum around that distance.

Figure 7 also shows (5 · 7) proportional to the ratio of the energies of the Sg- and Pg-wave after introducing the durations t_Δ of the wave trains:

$$\frac{(A_\Delta(Sg)/T_\Delta(Sg))^2\ t_\Delta(Sg)}{(A_\Delta(Pg)/T_\Delta(Sg))^2\ t_\Delta(Pg)} = \frac{v(Pg)}{v(Sg)} \left[\frac{k(Pg)}{k(Sg)}\right]^2 \frac{E_\Delta(Sg)}{E_\Delta(Pg)} \qquad (5 \cdot 7)$$

Here, six quantities determined experimentally are combined, four of them in the second power, and the scatter is considerable. The characteristic features found above, however, are confirmed. In particular, close to the epicenter the ratio (5 · 7) amounts to about 280. Taking into account the ratio of the velocities of Sg- and Pg-waves from table 1, i.e. 0.56, and the ratios (5 · 2) and (5 · 3), we find that close to the epicentre the S-wave energy is about 100 times that of the P-wave. The nearest epicentre had a distance of 14.4 km.

Consequently, in our epicentral distance range the Pg-wave energy can be disregarded in comparison with the Sg-wave energy for any calculation of seismic energy emitted by the earthquake focus.

Figure 8 shows the ratio (5 · 6) of the maximum Sg- and Pg-wave particle velocities for explosions in the distance range from 100 to 340 km. Only a slight increase with distarce is observed. Similar features are seen for the ratio (5 · 7) proportional to the energies (figure 8). Considering the ratio of the Sg- to Pg-velocity (5 · 2) and (5 · 3), as before, we see that the energy carried by the Sg-waves is still prevailing, but amounts in average to less than 3 times that carried by Pg-waves. This feature was used as one of the criteria to distinguish in some cases between earthquakes and explosions in the present investigation.

The ratio of the particle velocities for Sg- and Pg-waves was plotted as function of magnitude, as seen in figure 9. The scatter of the data is large, and no dependence of this ratio upon the earthquake magnitude can be concluded.

5.2. Attenuation of Sg-wave energy

If a relationship is found connecting the ratio $A_\Delta(Sg)/T_\Delta(Sg)$ with the epicentral distance Δ and the magnitude M_L, the attenuation of the Sg-wave can be found from recordings of a single station, just as well as of an array station.

Here, a dependence in the following form is assumed:

$$\log \left[\frac{A_\Delta(Sg)}{T_\Delta(Sg)} \Delta^n \right] = X + Y M_L \qquad (5 \cdot 8)$$

n, X, Y are constants.

The factor Δ^n accounts for both the geometrical spreading and the absorption. An attenuation according to Δ^n was found by Gutenberg

& Richter (1942), who noticed that

$$\frac{A_\Delta(Sg)}{T_\Delta(Sg)}\,\Delta^n \qquad (5\cdot 9)$$

with n=2 was constant for an earthquake with a certain magnitude, recorded at different distances. Lampson (1946) demonstrated that an expression of the form (5 · 9) is constant for explosions. The observed decrease of amplitude ranges from the inverse third power at short epicentral distances to an inverse first power at large distances. A number of numerial values was compiled by Howell (1963).

Theoretically it is more correct to express the attenuation in the form

$$\frac{A_\Delta(x)}{T_\Delta(x)} = \frac{A_h(x)}{T_h(x)}\,e^{-\alpha\Delta}\,\Delta^{-n} \qquad (5\cdot 10)$$

where α is the absorption coefficient and n is equal to 1 for body waves and $\frac{1}{2}$ for guided waves.

But if the amplitude $A_\Delta(x)$ is associated with the maximum amplitude at any distance, the term involving α in (5 · 10) is usually omitted, and both the geometric spreading and absorption are expressed by the exponent n, as in (5 · 8) (Howell 1963).

Differentiating (5 · 8) with respect to M_L, we find

$$Y = \frac{d\,\log\left[A_\Delta(Sg)/T_\Delta(Sg)\right]}{d\,M_L} \qquad (5\cdot 11)$$

to be independent of the exponent n for all distances where (5 · 8) is satisfied. Only the constant factor X will be affected by the exponent n.

By trial, we found the observational data to be best fitted by

n=2. No single X,Y-set, however, was acceptable for the entire magnitude and distance range. From figure 10a we have the following least square approximation for earthquakes and explosions in Arizona:

$$\log\left[\frac{A_\Delta(Sg)}{T_\Delta(Sg)}\Delta^2\right] = 7.183 + (0.890 \pm 0.026)\, M_L \qquad (5 \cdot 12)$$

in the magnitude range $-0.7 \leq M_L \leq +2.4$ and distance range 14 km $\leq \Delta \leq$ 340 km. From figure 10b we have for earthquakes in Imperial County and Baja California:

$$\log\left[\frac{A_\Delta(Sg)}{T_\Delta(Sg)}\Delta^2\right] = 6.941 + (0.804 \pm 0.018)\, M_L \qquad (5 \cdot 13)$$

in the magnitude range $+1.5 \leq M_L \leq +4.9$ and distance range 310 km $\leq \Delta \leq$ 640 km. A_Δ and Δ are given in cm, T_Δ in sec. Equations of this form are in good agreement with the equation for the perceptibilty limit (figure 3) at least for positive magnitudes.

Comparing the formulas (5 · 12) and (5 · 13) with (5 · 4) we notice that Sg-wave energy decreases with the 4th power of the distance. As the Sg-wave is a guided wave, the energy attenuation due to geometrical spreading is proportional to Δ ; the absorption of energy will thus be proportional to Δ^3.

Besides that, at an approximate distance of 325 km we observe a sudden increase of attenuation. A similar change in attenuation at an epicentral distance of somewhat above 300 km was found in other parts of the world (Bune & al. 1960, Kárník 1962). Therefore the discontinuity in attenuation, as seen from figure 10a,b, is unlikely to be caused by regional differences in the crustal structure between Arizona on one side and Imperial County and Baja California on the other. It is rather

the propagation mode of Sg-waves, which causes the discontinuity in the attenuation.

The sudden increase in attenuation at this distance is manifested by the decrease of X in (5 · 8), amounting to 0.41 at M_L = + 2.0 as seen from the formulas (5 ·12) and (5 ·13) and figure 10a,b. This corresponds to a decrease of the ratio $A_\Delta(Sg)/T_\Delta(Sg)$ by a factor of 2.57 or to a decrease of the energy of the Sg-wave nearly seven times. It seems probable that this is connected with the rapid increase in Sg-wave period at the distance of 300-350 km (figure 5).

The sudden increase of Sg-wave periods at a distance of 100 km (figure 5c) indicates another discontinuity in attenuation. Unfortunately, the data are too scanty for a direct estimate of the decrease in $A_\Delta(Sg)/T_\Delta(Sg)$ at this distance.

5.3 Seismic energy released in an earthquake

Knowing the attenuation and the duration of the Sg-wave as function of magnitude, the seismic energy released at the focus of an earthquake with magnitude M_L can be determined. We have from (5 · 4), neglecting the insignificant factor k(Sg):

$$\log E_h(Sg) = \log (2\pi^3 \rho v(Sg)) + 2 \log h + 2 \log \left[A_h(Sg)/T_h(Sg)\right] + \log t_h. \qquad (5 \cdot 14)$$

Taking ρ = 2.7 g/cm^3 (Gutenberg & Richter 1956a), assuming h = 14 km, v(Sg) = 3.25 km/sec (table 1), and substituting (4 · 1) and (5 · 12) with Δ = h = 14 km into (5 · 14), we obtain:

$$\log E_h(Sg) = 10.06 + (2.17 \pm 0.07)\, M_L \qquad (5 \cdot 15)$$

for the magnitude range $-0.7 \leq M_L \leq +2.4$ and distance range 14 km $\leq \Delta \leq$ 340 km. The attenuation formula (5 · 13) cannot be extrapolated to epicentral distances lower than 310 km without taking into account

the sudden increase in attenuation at about that distance. Compensation for that loss of seismic energy yields a magnitude-energy formula, practically equal to (5 · 15). Formula (5 · 15) is then valid in the magnitude range $-0.7 \leq M_L \leq +4.9$ and distance range 14 km $\leq \Delta \leq$ 640 km.

Although the magnitude of an earthquake is not affected by it, the discontinuity in attenuation between 300 km and 350 km causes a considerable difference of seismic energies recorded at two epicentral distances, slightly below and above this distance range.

It is of interest to compare the magnitude-energy formula (5 · 15) for local earthquakes with the corresponding formula for teleseisms:

$$\log E = 9.9 + 1.9\, M_L - 0.024\, M_L^2 \qquad (5 \cdot 16)$$

See Richter (1958, p. 366). We find that $E_h(Sg)/E$ is approximately 130 for $M_L = 5.0$, i.e. at a point where both formulas are expected to be valid. This may seem to be a large discrepancy whereas a comparison with an energy formula deduced from (5 · 13) gives almost perfect agreement ($E_h(Sg)/E = 6$). Still, it does not appear to be excluded that, at least in some cases, earlier energy estimates could be somewhat low because of insufficient information on the very high attenuation, especially of Sg, near the source (see Section 5.1).

6. DISCUSSION

TFSO is one of the most sensitive seismograph stations continuously operated. The effective increase of the sensitivity of a station entails that besides earthquakes a large number of artificial events is recorded, especially in regions with numerous quarries, like Arizona. This raises the problem of distinguishing between earthquakes and explosions in the range of small epicentral distances, up to

several degrees.

The appearance of an explosion record does not in general allow an immediate separation from an earthquake. This may be seen from the Arizona earthquakes reported in the TFSO-bulletin for the time interval Sep. 15, 1963 - Jan. 31, 1964. An arrangement of the reported events according to their origin time shows a clear maximum at about 4 p.m. local time, just before the working day is terminated and most explosions are fired. The maximum is equally well pronounced for reported California events, with the difference that the maximum occurs 1 hour later, due to the local time difference.

It is safest to separate explosion from earthquake records by knowing the explosion time and site.

From our investigation we found that the most pronounced difference between earthquakes and explosions is the ratio of S- to P-wave energy. The nearest recorded explosion had an epicentral distance of 100 km. It is surprising that the ratio of S- to P-wave energy amounts in average to as much as 5 (for earthquakes 10) and increases up to 10 (for earthquakes 40) at 300 km distance (figure 7). This allowed us to exclude explosions from the study of the Arizona seismicity.

The S-waves in explosions are unexpectedly strong if compared with the P-waves. However, they are weaker in explosions than in comparable earthquakes. This is in analogy to surface waves from nuclear explosions where Rayleigh waves dominate and Love waves are of secondary importance (Toksöz, Harkrider & Ben-Menahem 1964).

The discrimination of explosions and the study of local seismicity require accurate hypocentre determinations. For the epicentral distance and focal depth determination, local travel time tables of high precision are needed, giving the travel times even as function of azimuth. The accuracy in azimuth determination of an epicentre

from a single array station is limited mainly by the spacing within the array and by the appearance of phases at different epicentral distances. The azimuth is difficult to determine accurately from a single array station, especially at distances beyond about 3°, considering horizontal refractions in the crust and upper mantle. The conditions would certainly be very much improved if two or three array stations are situated at optimal relative distances. On the basis of the measurements presented in this paper, we find that a reasonable lower limit of the relative distance between two or more array stations equipped with seismometers like TFSO, is 3°: up to that distance the first events are sharp and the arrival times on different seismometers of the array can be determined with an accuracy up to 0.01 sec. The upper limit of the relative distance of two or more array stations depends on the lower magnitude limit of events desired to be recorded completely in number. From the perceptibility diagram (figure 3) it is seen that two or more array stations of TFSO-type, at a relative distance of 500 km would assure the number of earthquakes recorded to be complete down to magnitude +2.0 in the region between the stations.

The application of an array station to regional problems display some advantages as also shortcomings. The superiority of the seismographic array station over conventional stations results from:

(i) the high sensitivity of the single seismometers;

(ii) the possibility to improve the signal-to-noise ratio;

(iii) the regular spacing of seismometers;

(iv) the possibility to process the data automatically if recorded on magnetic tape;

(v) the convenience of operating the station limited to a relatively small site.

The main shortcoming of the array station if compared with a network of conventional stations, is the limitation in accuracy in

spite of the dimension of the array. This difficulty can be partially overcome by increasing the maximal dimension of the array, or better still, by using two or more array stations. Thereby each array can conveniently be composed of a simpler system of seismometers.

In our study the records from a selection of seismometers of TFSO were available on microfilm. Therefore the data could only be processed in the conventional way. Nevertheless, some new results on certain problems concerning the rheology of the earth's crust could be obtained.

From the perceptibility diagram (figure 3) we conclude that it is essentially impossible to record local earthquakes with small magnitudes at distances greater than some critical distance. No increase of the signal-to-noise ratio can improve this. The only possible way to include small local earthquakes seems to be to record them at small epicentral distances.

From a complete recording of earthquakes in two sequences down to very small magnitudes, the recurrence diagrams (figure 4) were found to have a break at a magnitude of about +3.7 such that the rate of increase of the number of earthquakes with decreasing magnitude becomes smaller for magnitudes below this limit. This raises the question whether further breaks occur at still smaller magnitudes.

In the light of this finding it seems problematic to extrapolate the recurrence diagram in any direction beyond the magnitude limits for which it has been found or to draw conclusions about the probable future occurrence of earthquakes. An extrapolation can be performed only if the coefficients in the recurrence formula (3 . 1) or (3 . 2) can be assumed to be constant also outside of the magnitude range investigated or if the change of these coefficients with magnitude is known None of these conditions is fulfilled and an extrapolation can only be speculative. Therefore, our results do not support an idea,

which has sometimes been expressed, that it would be possible to get a reliable information on long-term statistics of the seismicity of an area by recording a large number of very small shocks within a relatively limited time interval.

The attenuation of seismic waves may seem impossible to be studied from records of a single station, even an array station, since both the magnitude and epicentral distance change for every recorded earthquake. However, even in that problem the array station records have proved to deliver results comparable to those of a network of conventional stations. The propagation of seismic waves at shortest epicentral distances turned out to be complicated. The rapid increases of period at distances of 100 and about 325 km cause a sudden increase in the wave attenuation. This is especially clear for Sg-waves, carrying most of the seismic energy. The knowledge of the attenuation pattern allowed a better estimation of the seismic energy released in local earthquakes.

ACKNOWLEDGMENTS

This research was supported by the Contract AF-49(638)-1337 of the Air Force Office of Scientific Research Projects Agency Project VELA and the Contract AF 61(052)-588 of the Cambridge Research Laboratories of the Office of Aerospace Research, United States Air Force, through its European Office, as part of the Advanced Research Projects Agency's project VELA-UNIFORM.

I an very much indebted to Professor Markus Båth, Director of the Seismological Institute, Uppsala, for enabling me to travel to the United States and stay at the Seismological Laboratory in Pasadena, where the present investigation was performed. I wish to express to Professor Markus Båth my most sincere gratitude for encouragement

throughout the week and much helpful advice and valuable discussions, as also for assistance in framing the manuscript.

Professor Frank Press, Director of the Seismological Laboratory, Pasadena, proposed to me the subject of this investigation, supported it and contributed to it in a number of valuable discussions and read the first draft of the paper. I like to express to Professor Frank Press my deep appreciation for making possible my temporary stay at the Seismological Laboratory in Pasadena.

My best thanks are extended to Professor Ch. Richter, Professor Cl. Allen and Mr. L. Lenches, Pasadena, Mr. A.M. Rugg, Jr., Payson, Arizona, and Mr. B. Jansson, Uppsala, who contributed in various aspects of my research.

REFERENCES

Asada, T. 1957 Observations of nearby microearthquakes with ultra sensitive seismometers. J. Phys. Earth. 5, 83-113.

Båth, M. 1954 The elastic waves Lg and Rg along Euroasiatic paths. Arkiv f. Geof. 2, 295-342.

Båth, M. 1962 Channel waves in the earth's continental crust. Scientia, 56ème Année, 1-8.

Berg, J.W. Jr., Cook K.L., Narans H.D. & Dolan W.M. 1960 Seismic investigation of crustal structure in the eastern part of the Basin and Range Province. Bull. Seism. Soc. Am. 50, 511-36.

Bune, V.I., Gzovskij M.V. et al. 1960. Methods for a detailed study of seismicity. Trudy Inst. Fiz. Zemli im. O.Yu. Smidta, English Translation No. 9 (176).

Diement W.H., Steward S.W. & Roller J.C. 1961 Crustal structure from the Nevada test site to Kingman, Arizona, from seismic and gravity observations. J. Geoph. Res. 66, 201-14.

Eardley A.J. 1951 Structural Geology of North America. Harper Brothers, New York.

Gutenberg B. & Richter C.F. 1942 Earthquake magnitude, intensity, energy, and acceleration. Bull. Seism. Soc. Am. 32, 163-92.

Gutenberg B. & Richter C.F. 1954 Seismicity of the Earth and associated Phenomena. Princeton University Press.

Gutenberg B. & Richter C.F. 1956a Earthquake magnitude, intensity, energy, and acceleration. Bull. Seism. Soc. Am. 46, 105-46.

Gutenberg B. & Richter C.F. 1956b Magnitude and energy of earthquakes. Ann. di Geof. IX, 1-15.

Howell Jr. B.F. 1963 Absorption of seismic waves. VESIAC State-of-the-Art Report, The University of Michigan.

Jeffreys H. 1931 On the cause of oscillatory movement in seismograms. Month. Not. R.A.S., Geoph. Supplement II, No. 8, 407-16.

Jeffreys H. & Bullen K.E. 1958 Seismological Tables, Brit. Assoc. Advanc. Science, London.

Kárník V. 1962 Amplitude-distance curves of surface waves at short epicentral distances (Δ < 2000 km). Studia Geoph. et Geodet. 4, 340-46.

Lampson C.W. 1946 Final report on effects of underground explosions. Nat. Def. Res. Comm. of the Office of Sci. Res. and Dev., Report No. A-479.

Pakiser L.C. 1963 Structure of the crust and upper mantle in the western United States. J. Geoph. Res. 68, 5747-56.

Pakiser L.C. & Hill D.P. 1963 Crustal structure in Nevada and southern Idaho from nuclear explosions. J. Geoph. Res. 68, 5757-66.

Press F. 1960 Crustal structure in the California-Nevada region. J. Geoph. Res. 65, 1039-51.

Press F. & Ewing M. 1952 Two slow surface waves across North America. Bull. Seism. Soc. Am. 42, 219-28.

Press F. & Gutenberg B. 1956 Channel waves Ng in the earth's crust. Trans. Am. Geoph. Union 37, 754-56.

Richter C.F. 1935 An instrumental earthquake magnitude scale. Bull. Seism. Soc. Am. 25, 1-32.

Richter C.F. 1958 Elementary Seismology. W.H. Freeman & Co., San Francisco.

Sanford A.R. & Holmes C.R. 1962 Microearthquakes near Socorro, New Mexico. J. Geoph. Res. 67, 4449-59.

Tatel H.E. 1954 Note on the nature of a seismogram II. J. Geoph. Res. 59, 289-94.

Tatel H.E. & Tuve M.A. 1954 Note on the nature of a seismogram I. J. Geoph. Res. 59, 287-88.

Tatel H.E. & Tuve M.A. 1955 Seismic exploration of a continental crust. Geol. Soc. Am. Spec. Paper 62, 35-50.

Toksöz M.N., Harkrider D.G. & Ben-Menahem A. 1964 Determination of source parameters by amplitude equalization of seismic surface waves; 2. Release of tectonic strain by underground nuclear explosions and mechanism of earthquakes (in print).

Townley S.D. & Allen M.W. 1939 Descriptive catalog of earthquakes of the Pacific Coast of the United States 1769-1928. Bull. Seism. Soc. Am. 29, 1-297.

Utsu T. 1961 A statistical study on the occurrence of aftershocks. The Geoph. Mag. 30, 521-606.

Woollard G.P. 1951 Report of the Special Commitee on the geophysical and geological study of continents 1950-51. Trans. Am. Geoph. Union 32, 634-47.

Table 1. Results from earthquakes for which USCGS information was available.

Date 1963	GMT	Δ Km	(i) Pn velocity km/sec	(i) Sn velocity km/sec	(ii) Pn velocity km/sec	(ii) Sn velocity km/sec	σ J.-B.	σ J.-B.	Pg velocity km/sec	Sg velocity km/sec	σ J.-B.	σ J.-B.	P* velocity km/sec	M_L Pas	M_L TFSO	M_L(Pas)-M_L(TFSO)
Arizona																
Nov. 2	08 47 43.4	281	7.80±		8.20± [1]					3.06				+4.0	+3.7	+0.3
Imperial County California																
Oct. 27	14 50 19.7	395	7.53		7.80				5.70	3.15				+4.2	overshoot	
	14 56 55.0	410	7.70		8.00					3.42			6.05	+4.1	+3.9	+0.2
	15 24 10.6	395	7.60		7.95				5.84	3.25				+3.4	+3.0	+0.4
	15 30 43.4	410	7.90	4.50	8.38	4.80	0.26	0.26		3.37			6.09	+3.4	+3.5	-0.1
	18 07 44.4	395	7.50		7.93				5.76	3.23			6.47	+4.0	+3.8	+0.2
	18 12 49.2	404	7.60		7.95				5.91	3.18			6.58	+2.4	overshoot	
	18 22 05.3	421	7.86		8.20				5.78	3.40			6.19	+3.9	+3.4	+0.5
	18 49 36.3	395	7.60		7.95				5.84	3.03				+3.9	+3.8	+0.1
			7.66 ±0.14	4.50±	8.02 ±0.17	4.80±			5.81 ±0.07	3.25 ±0.13	0.21	0.20	6.28 ±0.21			+0.2
Baja California																
Nov. 23	07 50 46.3	533	8.30		8.60					3.33				+6.0	overshoot	
	08 17 16.6	533	8.20		8.50				5.57	3.43					+4.2	
	08 32 30.9	544	8.20		8.50					3.51				+5.0±	+4.9	+0.1
	08 47 17.4	586	8.40		8.60					3.41					+4.9	
	10 20 10.2	533	8.80		9.05					3.37					+4.0	
	10 53 18.4	473	8.20		8.50				5.16	2.99					+3.7	
			8.35 ±0.21		8.63 ±0.18				5.37 ±0.20	3.34 ±0.17	0.19	0.21				+0.1±

1) computed on the assumption of a Pg-velocity equal to that from Imperial County. (i), (ii) see Section 4.1 .

Table 2. Corresponding phase symbols at different distances.

Epicentral distances of about			
$\leq 6^{o}$	$\geq 6^{o}$	$\leq 6^{o}$	$\geq 6^{o}$
Pn	Pn corresponds to	Sn	Sn
P* probably identical with	Lg corresponds to		Lg1
Pg	Pg corresponds to	Sg identical with	Lg2

Table 3. Least-square solutions for period-distance relations (figure 5): $T(x) = a + b\Delta$, with T in sec and Δ in km.

x	Δ	a	$b \times 10^{+4}$	Correlation between T and Δ
Pn	100-800	0.23	$+ 2.2 \pm 0.3$	+ 0.17
	100-300	0.27	$- 1.6 \pm 1.2$	0.02
	300-800	0.44	$- 1.6 \pm 0.6$	0.05
Pg	14-640	0.14	$+ 6.6 \pm 0.4$	0.58
	14-100	0.14	$+ 8.6 \pm 3.6$	0.16
	100-300	0.20	$+ 2.5 \pm 1.1$	0.05
	300-640	0.19	$+ 5.7 \pm 1.3$	0.16
Sg	14-640	0.11	$+ 12.1 \pm 0.6$	0.64
	14-100	0.19	$+ 0.3 \pm 4.6$	0.00
	100-300	0.34	$- 0.4 \pm 2.5$	0.00
	300-640	- 0.24	$+ 19.8 \pm 1.4$	+ 0.57

Figure Captions

Figure 1. Epicentral map of Arizona for earthquakes in the time interval Sep. 15, 1963-Jan. 31, 1964, Imperial County, California, for earthquakes on Oct. 27, 1963, and Baja California, for earthquakes on Nov. 23-31, 1963.

Figure 2. Response characteristics for a) Johnson-Matheson array seismometer, and b) standard Wood-Anderson torsion seismometer.

Figure 3. Perceptibility diagram.

Figure 4. Recurrence diagram. The right-hand scale refers to Imperial County.

Figure 5. Period versus epicentral distance of Pn-waves, Pg-waves and Sg-waves. f = frequency = 1/T.

Figure 6. Duration of Sg-phase as function of magnitude.

Figure 7. Ratios $A_\Delta(Sg)/T_\Delta(Sg)$: $A_\Delta(Pg)/T_\Delta(Pg)$ and $(A_\Delta(Sg)/T_\Delta(Sg))^2\ t_\Delta(Sg)$: $(A_\Delta(Pg)/T_\Delta(Pg))^2\ t_\Delta(Pg)$ for earthquakes versus distance.

Figure 8. Ratios $A_\Delta(Sg)/T_\Delta(Sg)$: $A_\Delta(Pg)/T_\Delta(Pg)$ and $(A_\Delta(Sg)/T_\Delta(Sg))^2\ t_\Delta(Sg)$: $(A_\Delta(Pg)/T_\Delta(Pg))^2\ t_\Delta(Pg)$ for explosions versus distance.

Figure 9. Ratio $A_\Delta(Sg)/T_\Delta(Sg)$: $A_\Delta(Pg)/T_\Delta(Pg)$ for earthquakes versus magnitude.

Figure 10. Attenuation for a) earthquakes and explosions in Arizona, b) earthquakes in Imperial County and Baja California. CGS-units are used.

Fig. 1

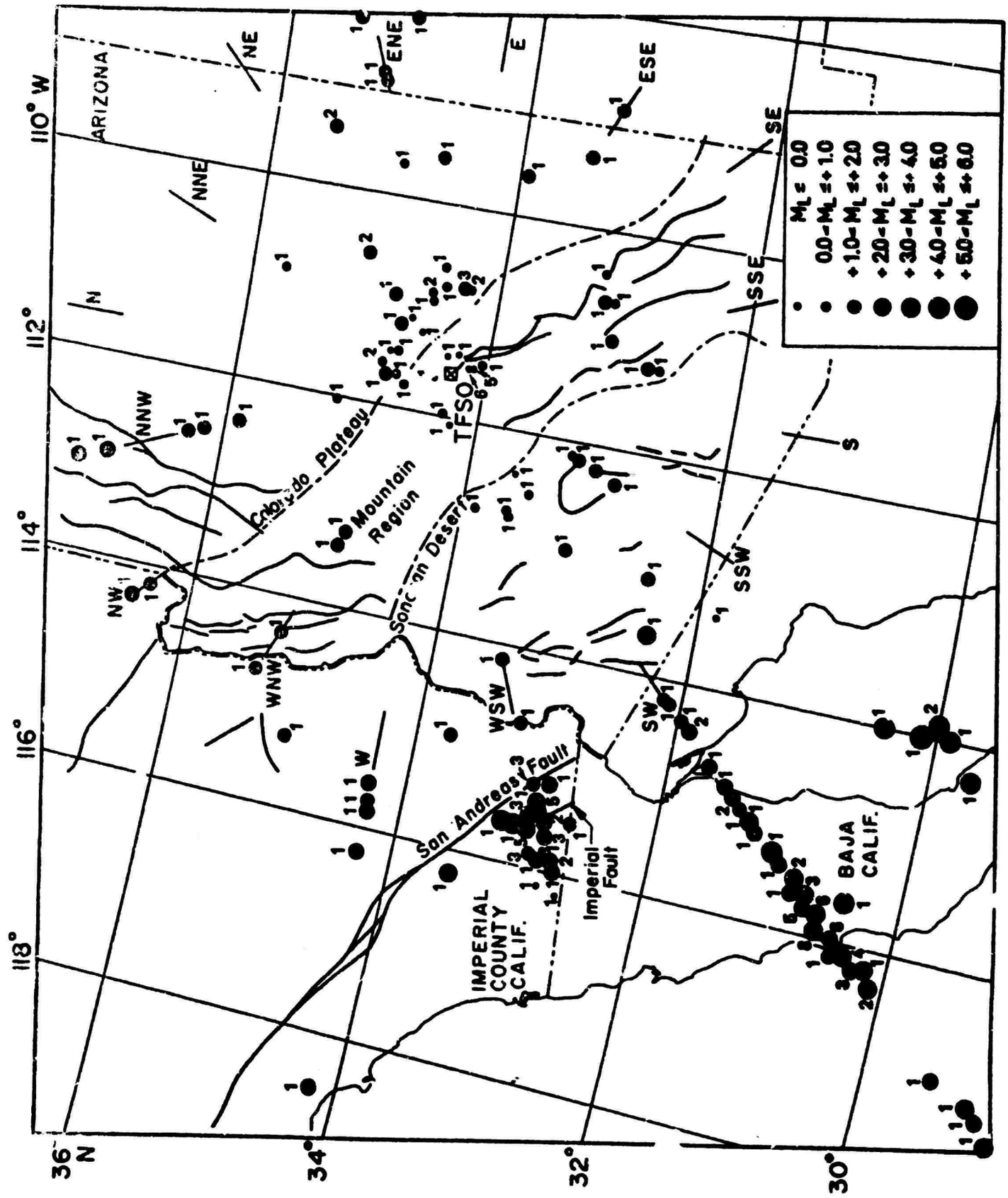
110° W
112°
114°
116°
118°
36° N
34°
32°
30°
ARIZONA
NE
ENE
E
ESE
SE
SSE
S
SSW
SW
WSW
W
WNW
NW
NNW
N
NNE
$M_L \leq 0.0$
$0.0 < M_L \leq 1.0$
$1.0 < M_L \leq 2.0$
$2.0 < M_L \leq 3.0$
$3.0 < M_L \leq 4.0$
$4.0 < M_L \leq 5.0$
$5.0 < M_L \leq 6.0$
TFSO
Colorado Plateau
Mountain Region
Sonoran Desert
San Andreas Fault
Imperial Fault
IMPERIAL COUNTY CALIF.
BAJA CALIF.

Fig. 2

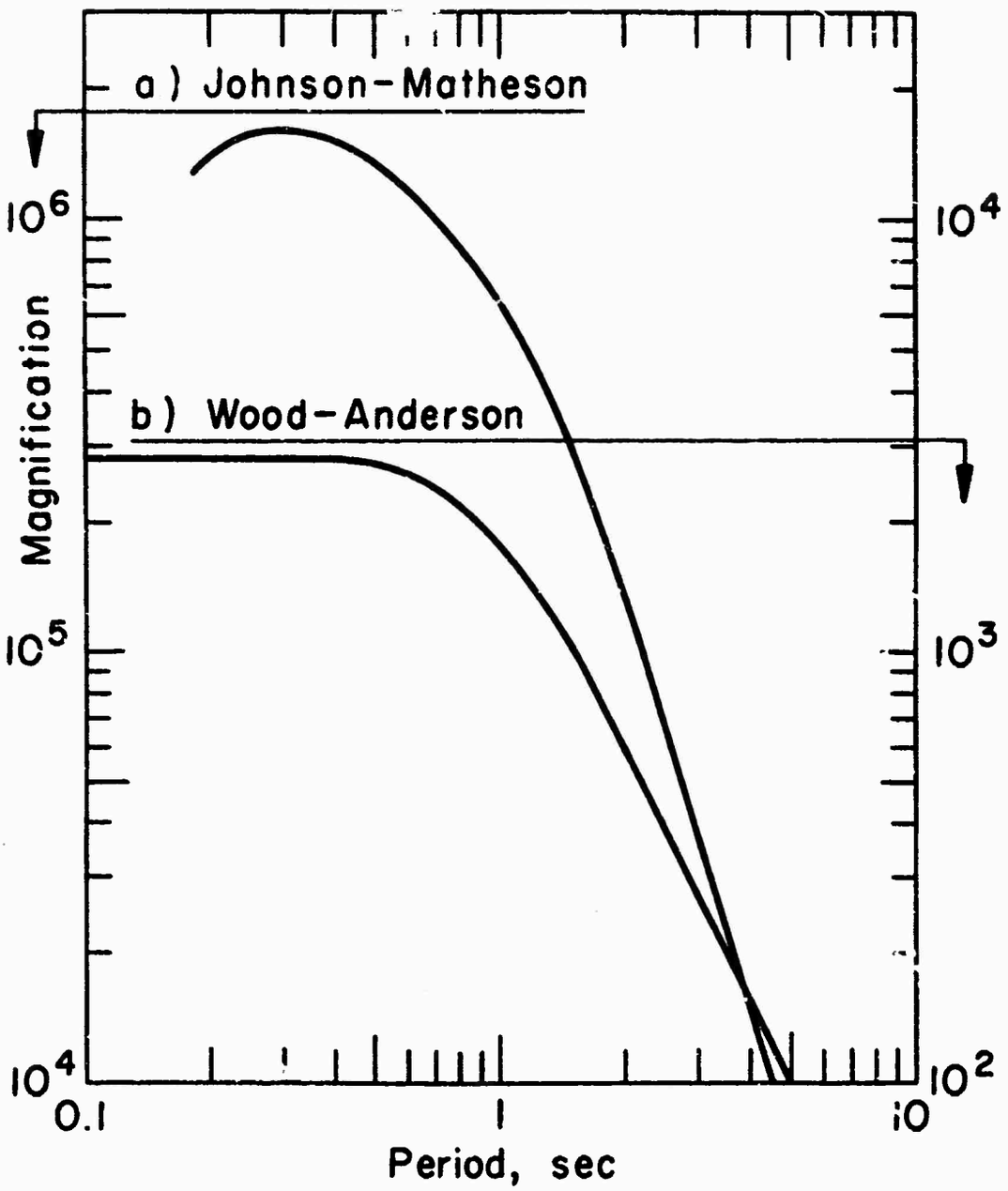
a) Johnson-Matheson
b) Wood-Anderson
Magnification
10^6
10^5
10^4
10^4
10^3
10^2
0.1
1
10
Period, sec

Fig. 3

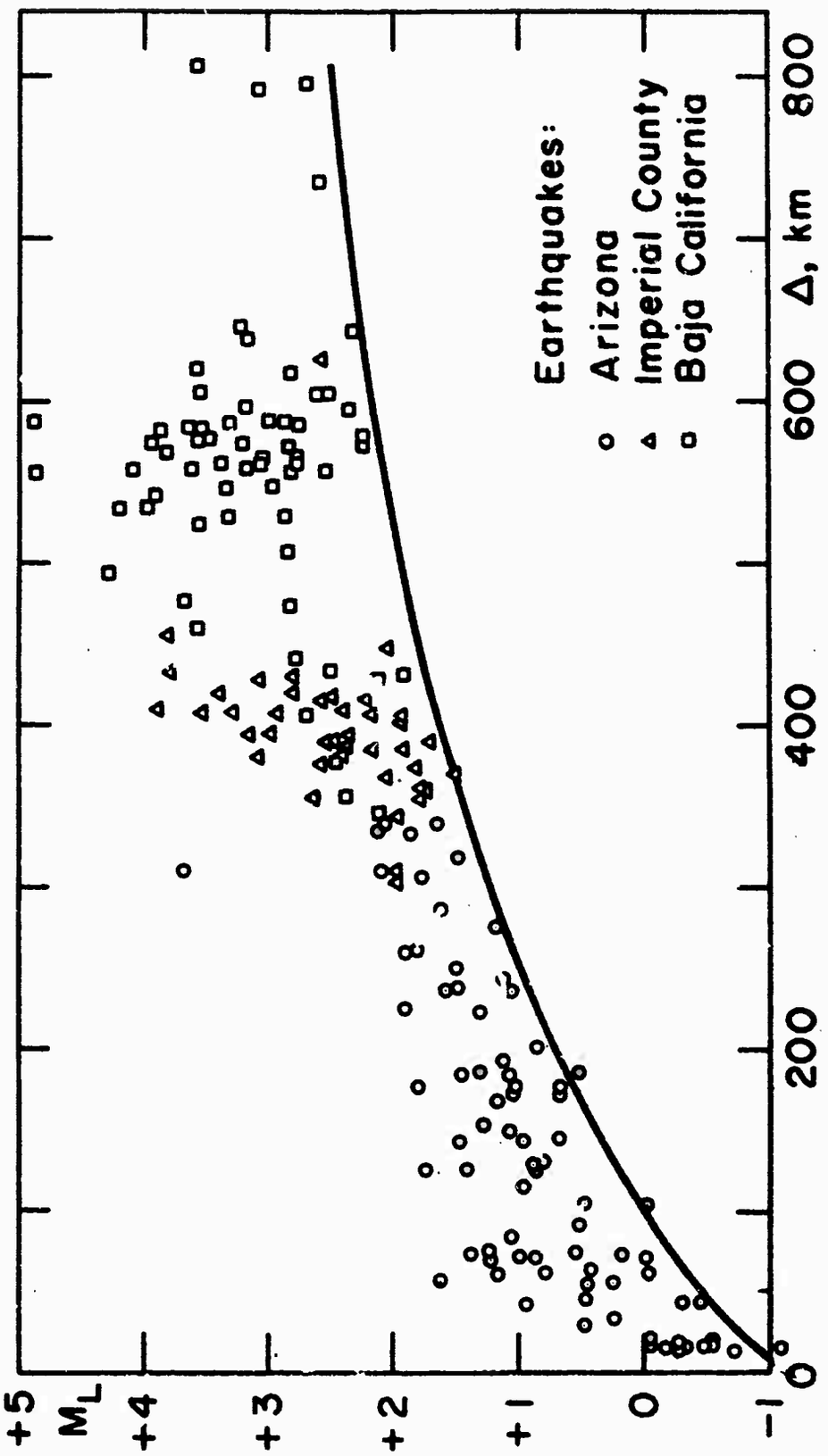
Earthquakes:
Arizona
Imperial County
Baja California
M_L
+5
+4
+3
+2
+1
0
-1
0
200
400
600
800
Δ, km

Fig. 4

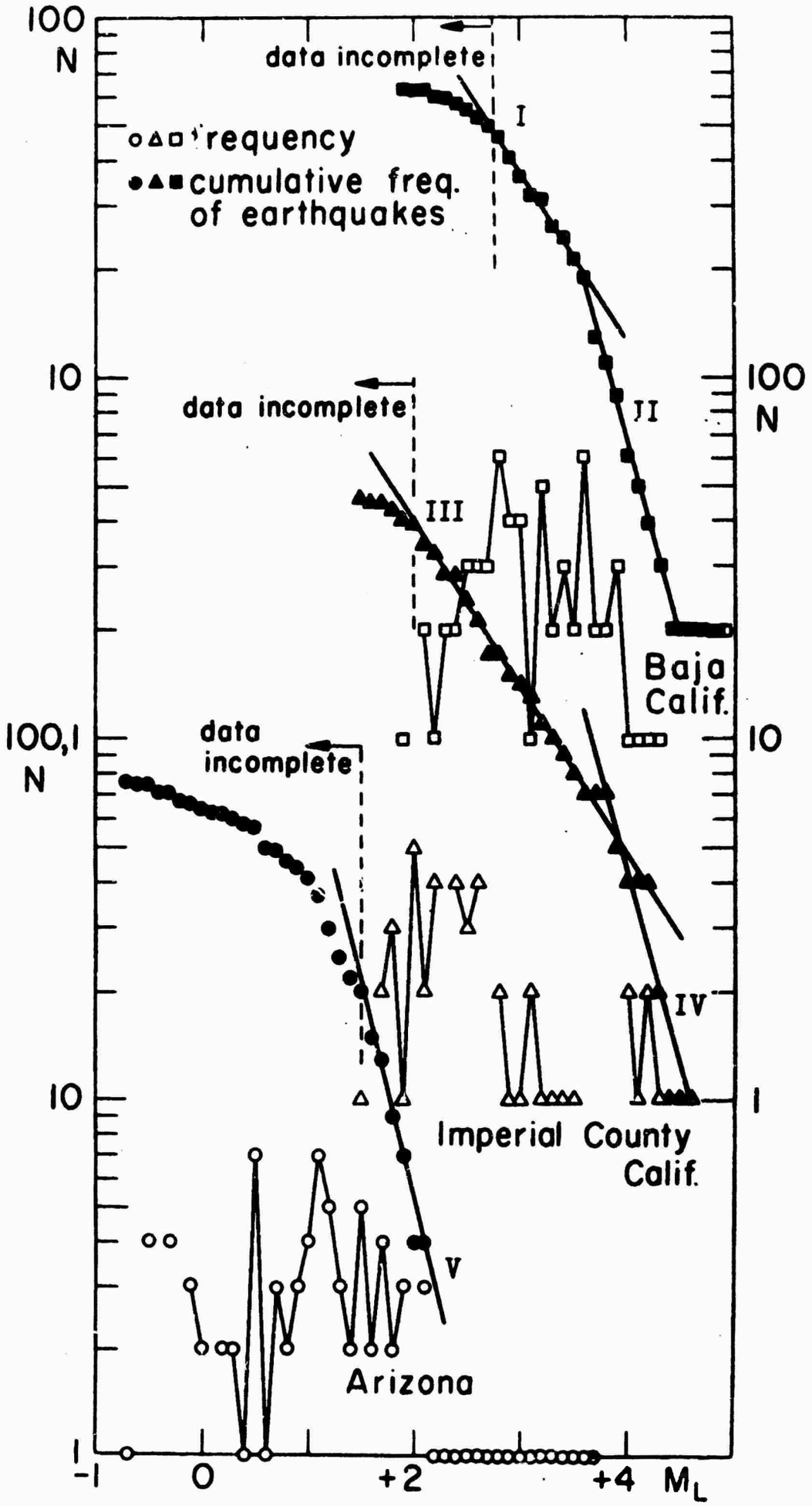
100
N
data incomplete
I
frequency
cumulative freq.
of earthquakes
10
data incomplete
II
100
N
III
Baja
Calif.
100,1
N
data
incomplete
10
IV
10
1
Imperial County
Calif.
V
Arizona
1
-1
0
+2
+4
M_L

Fig. 5

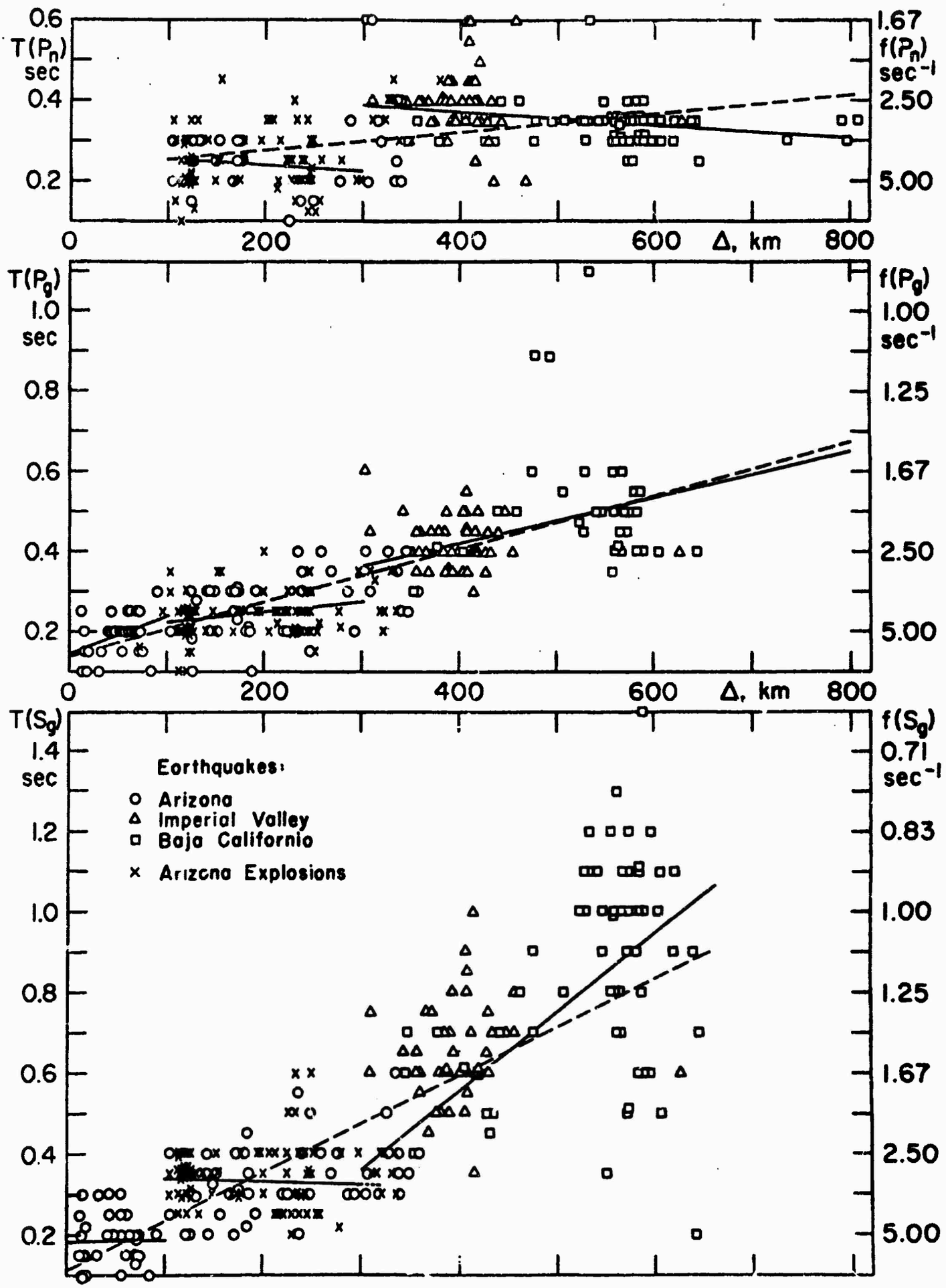
T(Pn) sec
f(Pn) sec⁻¹
0.6
0.4
0.2
1.67
2.50
5.00
0
200
400
600
800
Δ, km
T(Pg) sec
f(Pg) sec⁻¹
1.0
0.8
0.6
0.4
0.2
1.00
1.25
1.67
2.50
5.00
T(Sg) sec
f(Sg) sec⁻¹
1.4
1.2
1.0
0.8
0.6
0.4
0.2
0.71
0.83
1.00
1.25
1.67
2.50
5.00
Earthquakes:
Arizona
Imperial Valley
Baja California
Arizona Explosions

Fig. 6

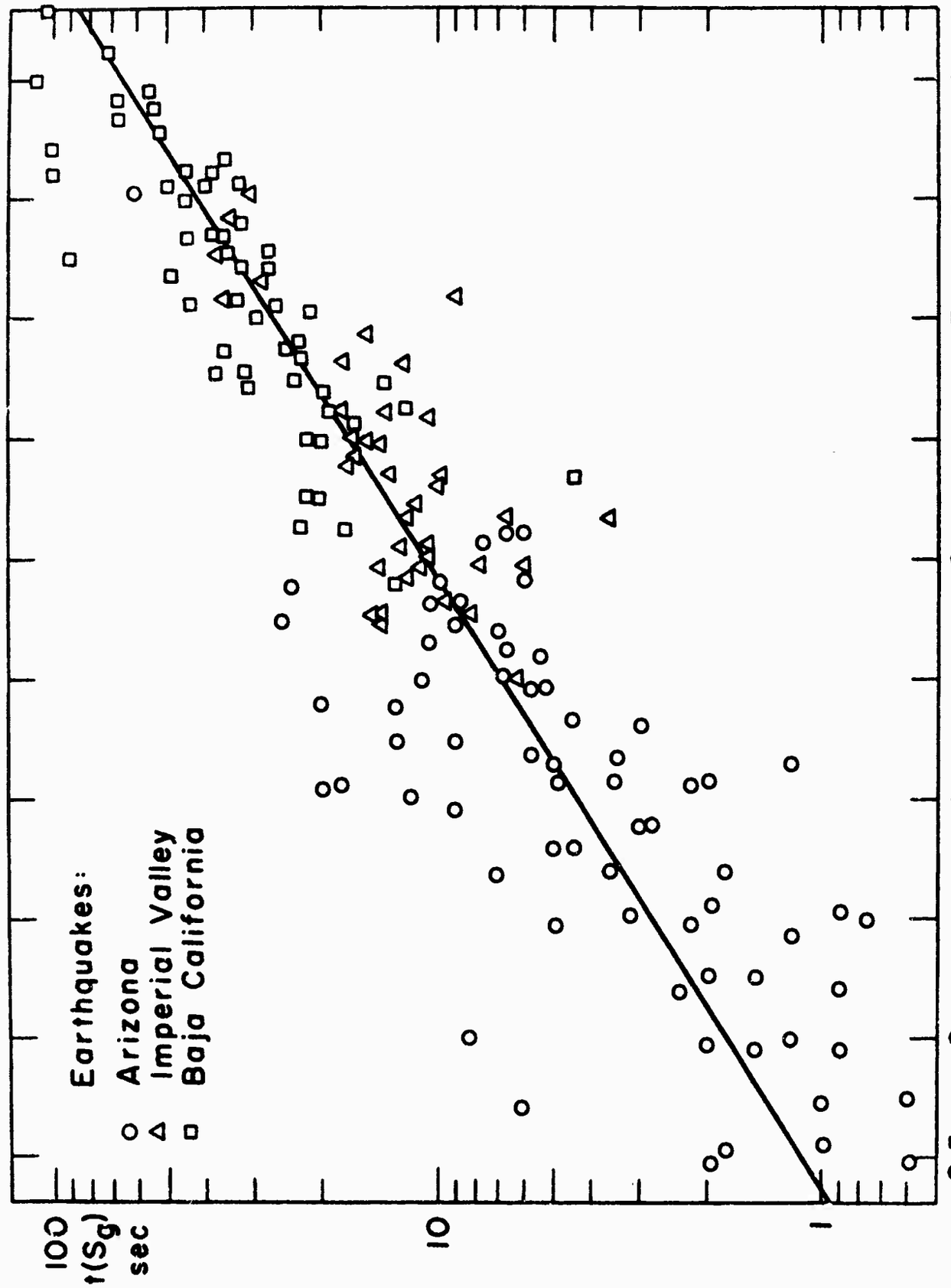
100
τ(Sg)
sec
10
1
-0.5
0
+1
+2
+3
+4
ML
Earthquakes:
Arizona
Imperial Valley
Baja California

Fig. 7

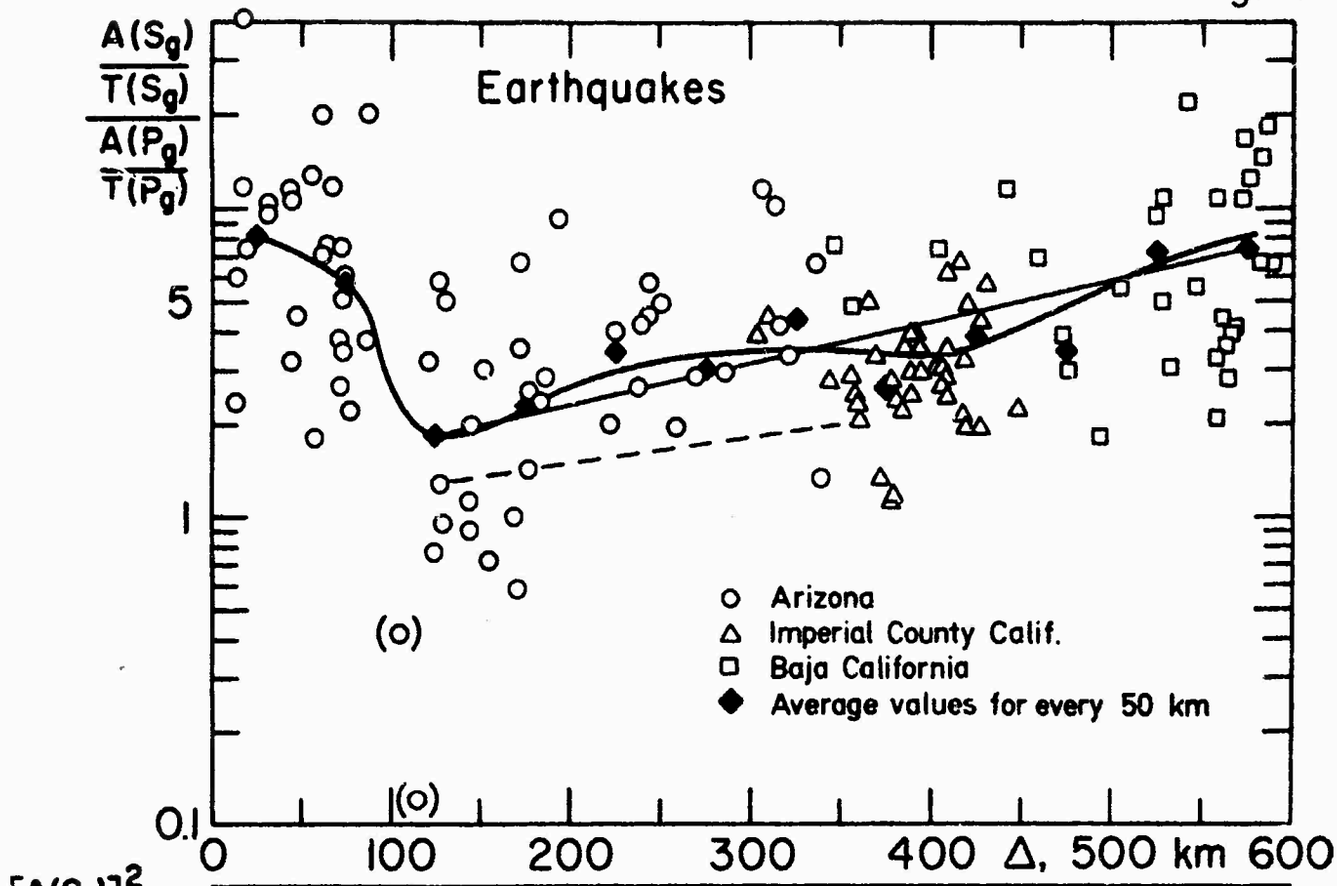
$\frac{A(S_g)}{T(S_g)} \Big/ \frac{A(P_g)}{T(P_g)}$
Earthquakes
5
1
0.1
(o)
Arizona
Imperial County Calif.
Baja California
Average values for every 50 km
0
100
200
300
400
Δ, 500 km
600

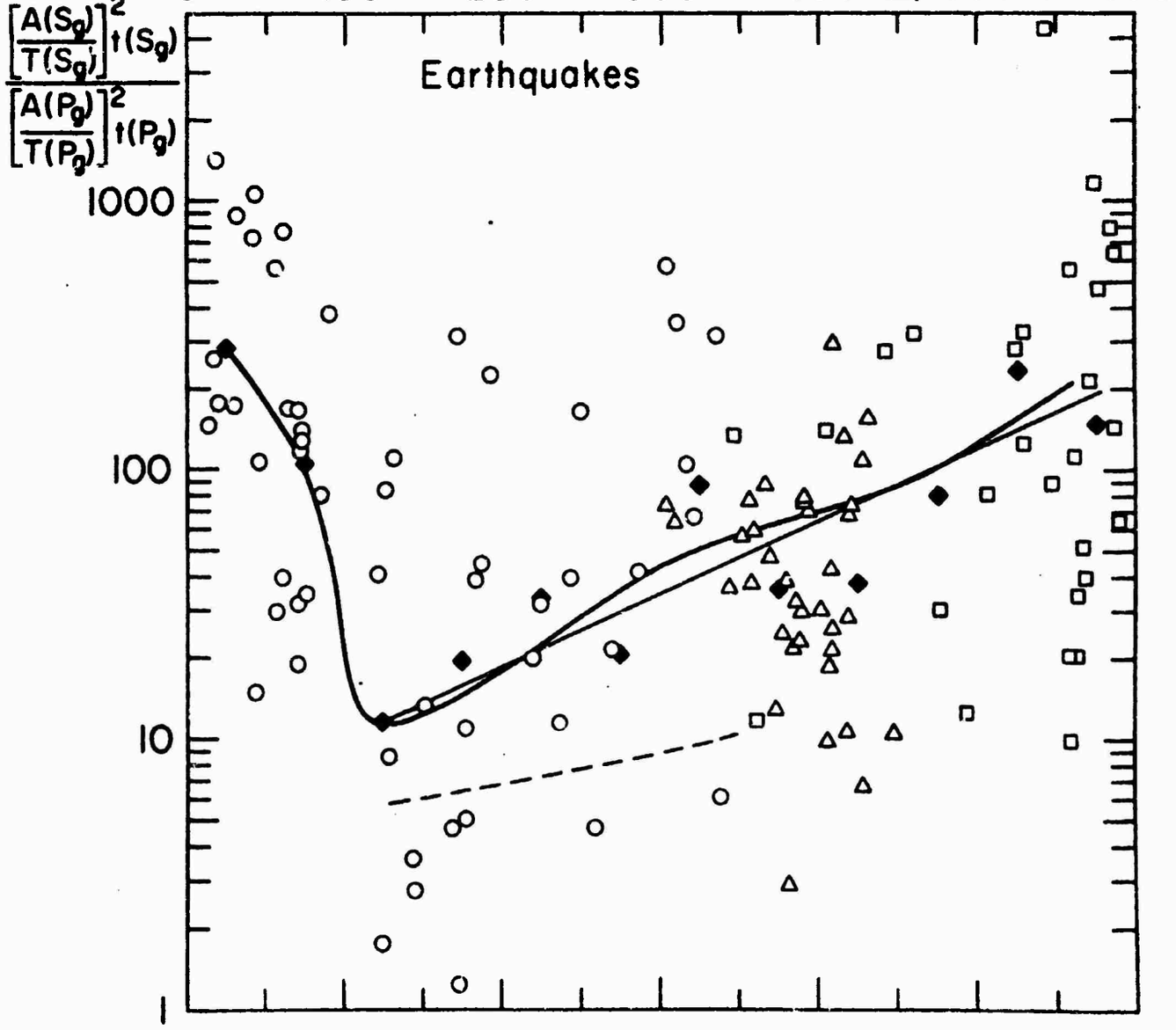
$\left[\frac{A(S_g)}{T(S_g)}\right]^2 t(S_g) \Big/ \left[\frac{A(P_g)}{T(P_g)}\right]^2 t(P_g)$
Earthquakes
1000
100
10
1

Fig. 8

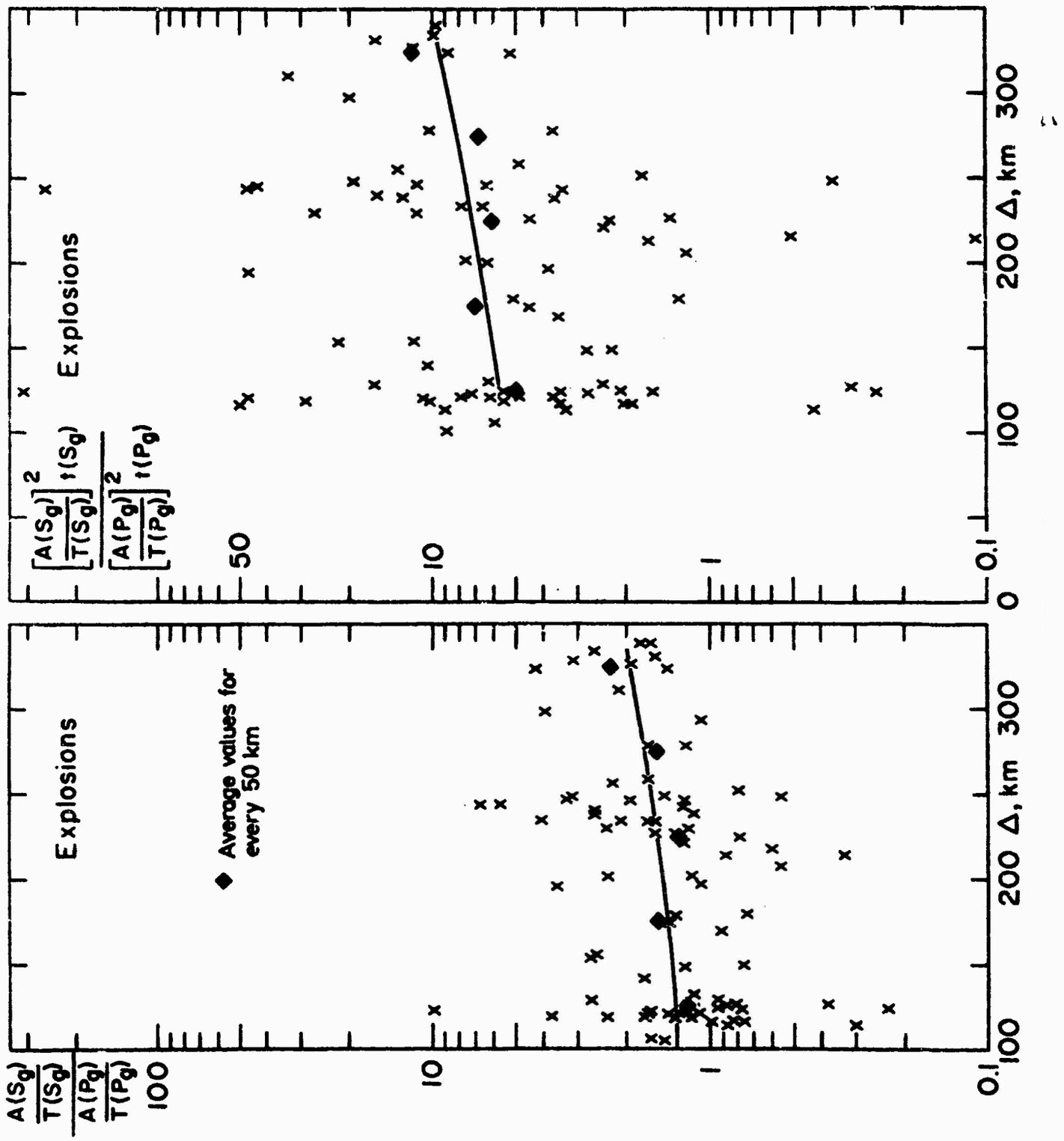
Explosions
Average values for every 50 km
Explosions
200 Δ, km 300
100
0.1
10
1
50
0
A(Sg)/T(Sg) / A(Pg)/T(Pg)
[A(Sg)/T(Sg)]² t(Sg) / [A(Pg)/T(Pg)]² t(Pg)

Fig 9

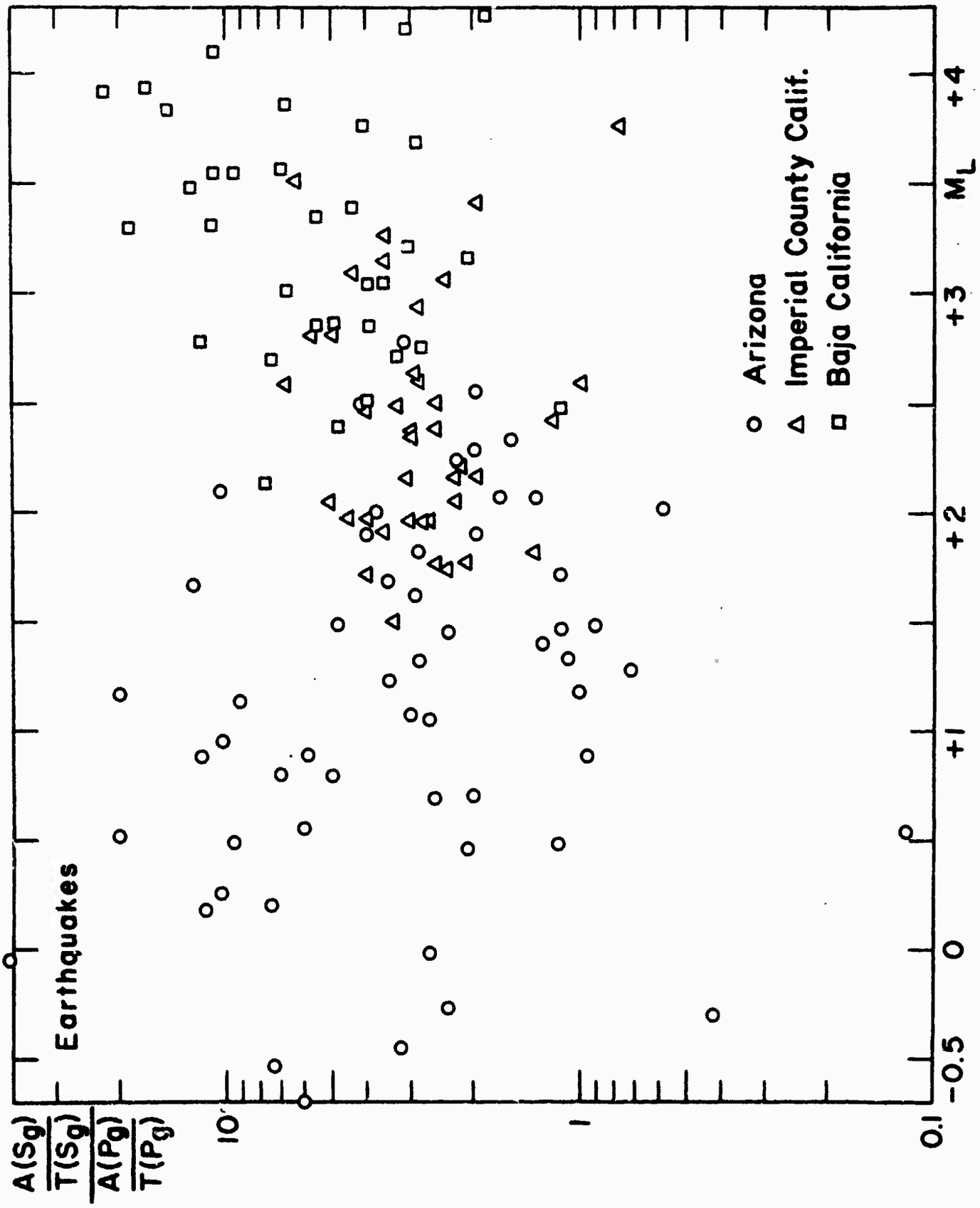
Earthquakes
Arizona
Imperial County Calif.
Baja California
$\frac{A(Sg)}{T(Sg)} / \frac{A(Pg)}{T(Pg)}$
10
1
0.1
-0.5
0
+1
+2
+3
+4
M_L

Fig. 10

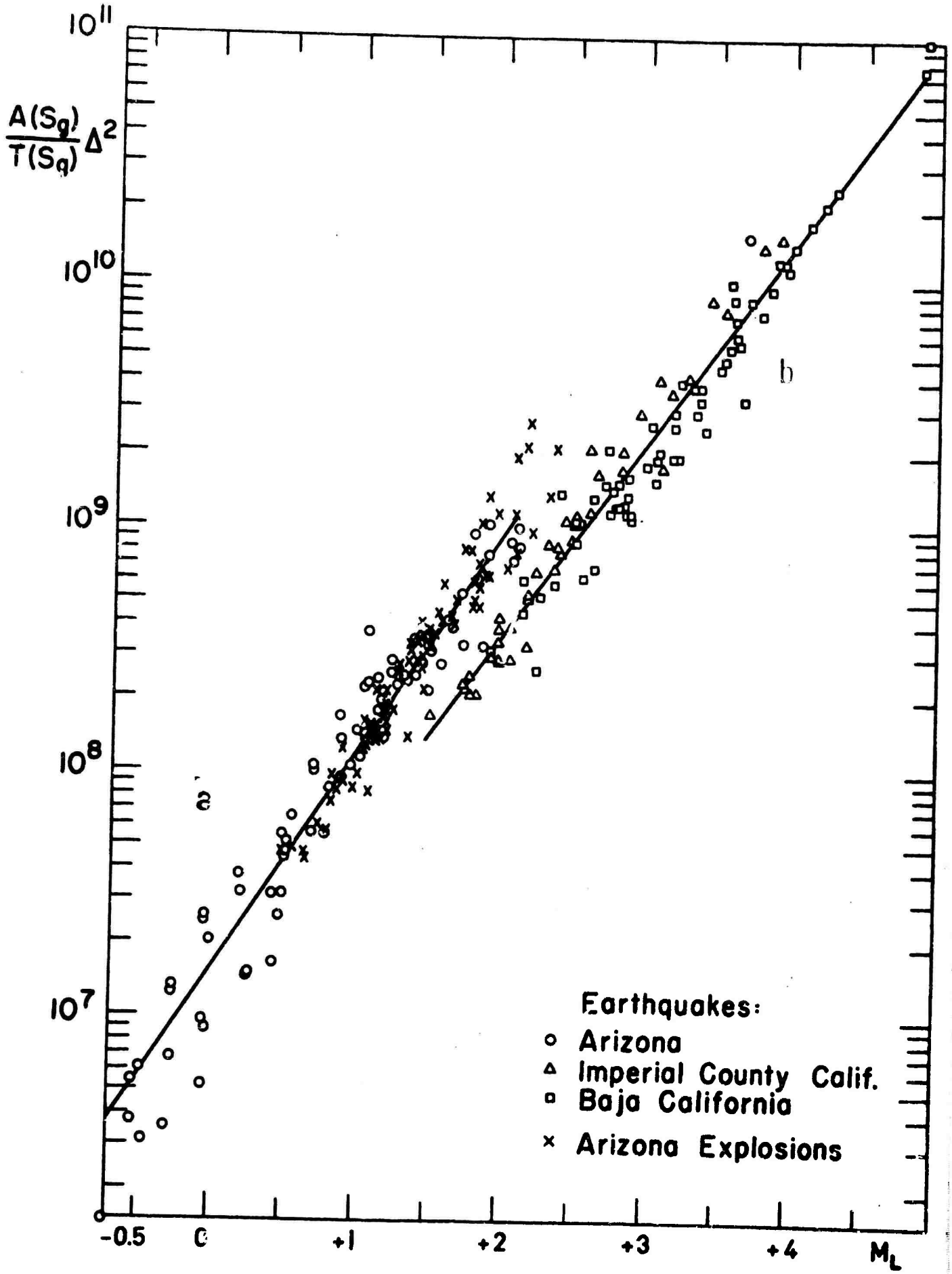
10^{11}
$\frac{A(S_g)}{T(S_g)}\Delta^2$
10^{10}
10^9
10^8
10^7
b
a
Earthquakes:
Arizona
Imperial County Calif.
Baja California
Arizona Explosions
-0.5
0
+1
+2
+3
+4
M_L